Biogeosciences, 23, 4057–4081, 2026
https://doi.org/10.5194/bg-23-4057-2026

Biogeosciences Open Access EGU

DOM consumption and demethylation of MeHg as potential drivers of low MeHg in Mediterranean Sea sponges and benthic fish: a modeling perspective

David J. Amptmeijer[1], Ulrike Hanz[2], Corinna Schrum[1,3], and Johannes Bieser[1]

[1]Matter Transport and Ecosystem Dynamics, Helmholtz-Zentrum Hereon, Geesthacht, Germany
[2]Benthic Ecology, Alfred Wegener Institute, Am Alten Hafen 26, 27568 Bremerhaven, Germany
[3]Universität Hamburg, Institute for Marine Sciences, Mittelweg 177, 20146 Hamburg, Germany

Correspondence: David J. Amptmeijer (davidamptmeijer@gmail.com)

Received: 30 October 2025 – Discussion started: 12 November 2025
Revised: 21 March 2026 – Accepted: 23 March 2026 – Published: 22 June 2026

Abstract. Methylmercury (MeHg) is a bioaccumulative neurotoxin that poses a risk to human health through seafood consumption. Sponges have unique mercury (Hg) profiles. Measurements show an unusually high inorganic Hg (iHg) content in Low Microbial Abundance (LMA) sponges and an even higher iHg content in High Microbial Abundance (HMA) sponges, while MeHg concentrations remain low, particularly in HMA sponges. Combined with the recently improved understanding of the important ecological role of sponges as a food source for other biota, this suggests that their low MeHg content may influence MeHg transfer within benthic food webs. In this study, we used a 1D water-column model to investigate the bioaccumulation of MeHg in sponges. It has been hypothesized that the low MeHg content in HMA sponges may result from active MeHg demethylation. Our model results indicate that the consumption of dissolved organic matter (DOM) can already explain the low observed MeHg content in LMA sponges, and higher DOM consumption in HMA sponges can account for the even lower MeHg levels in HMA species. Alternatively, if MeHg demethylation occurs, a low rate of $1\,\%\,d^{-1}$ could explain the differences between LMA and HMA sponges. Although DOM consumption increases iHg bioaccumulation in both sponge types, it does not explain the extremely high iHg concentrations observed. Finally, our model suggests that HMA sponges could potentially reduce MeHg concentrations in benthic fish by up to 53 % when they dominate at the base of the food web. These findings highlight the potentially important role of sponges in Hg cycling and indicate that sponge-dominated systems could help reduce MeHg accumulation in benthic food webs.

1 Introduction

Mercury (Hg) and methylmercury (MeHg) are both toxic pollutants that can bioaccumulate throughout the food chain (Mason et al., 1995). Although both Hg and MeHg can bioaccumulate, MeHg has a much higher bioaccumulation potential and greater toxicity (Jeong et al., 2024). MeHg bioaccumulates especially in high-trophic-level fish, which pose health risks to humans when consumed. But how ecosystem dynamics at the base of the food web influence MeHg bioaccumulation is poorly understood. In commercially important species such as Mediterranean bluefin tuna (*Thunnus thynnus*), Hg concentrations can increase by up to 8 orders of magnitude compared to seawater levels (Storelli et al., 2002; Tseng et al., 2021). Consumption of MeHg-polluted fish causes adverse health effects in humans and is estimated to cost the European Union up to EUR 8–9 billion per annum, mostly due to the loss of intelligence in children (Bellanger et al., 2013). Furthermore, Hg pollution leads to reduced fish stocks and restrictions on fishing practices, which can decrease supply and profitability in the fishing sector (Pacyna et al., 2006).

The primary pathway of MeHg bioaccumulation in aquatic ecosystems is direct uptake from the water column via respiration, diffusion, or ingestion. When this uptake results in

organism concentrations exceeding those in the surrounding water, the process is termed bioconcentration. This occurs because MeHg binds strongly to organic matter, particularly thiol (-SH) groups in proteins (Hao et al., 2022), increasing internal concentrations by 10^5–10^6-fold relative to water (Lee and Fisher, 2016). Bioconcentration is surface-area dependent and thus especially efficient in small organisms, making it critical at the base of the food web (Mason et al., 1995). Efficient trophic transfer of bioconcentrated MeHg results in increasing concentrations with trophic position, a process known as biomagnification. This typically increases MeHg bioaccumulation 3–10-fold per trophic level (Mason et al., 1996; Lavoie et al., 2013). This drives high MeHg levels in top predators, including human-consumed seafood. This means that the MeHg concentration at the base of the food web strongly influences bioaccumulation in higher trophic levels, making processes at the base of the food web critical for understanding ecosystem-wide MeHg dynamics. Since sponges are actively consumed by higher trophic levels and can dominate benthic biomass (Mortimer et al., 2021), unique MeHg accumulation patterns in sponges, compared to those in other megabenthos, could influence seafood contamination levels.

Unlike most marine food webs that are based on primary producers, sponges can utilize dissolved organic matter (DOM) as a food source. Because DOM strongly influences Hg speciation and bioavailability, this alternative trophic pathway may fundamentally alter MeHg uptake at the base of the food web. Since sponges are actively consumed by higher trophic levels and can dominate benthic biomass (Mortimer et al., 2021), unique MeHg accumulation patterns in sponges compared to other megabenthos could influence seafood contamination levels.

1.1 The ecological role of sponges

The base of most marine food webs is primary producers, but not all trophic chains start with living phytoplankton. Some animals, in particular sponges, can utilize Dissolved Organic Material (DOM) as a food source (De Goeij et al., 2013). The DOM uptake in sponges can be facilitated by bacterial symbionts. While all sponges have bacterial symbionts, there is a strong distinction between High-Microbial-Assemblage (HMA) sponges and Low-Microbial-Assemblage (LMA) sponges. HMA sponges can have 10^8 to 10^{10} bacteria g^{-1} sponge, whereas LMA sponges have 10^5 to 10^6 bacteria g^{-1} sponge, which is roughly equivalent to the concentration of bacteria in seawater (Hentschel et al., 2012). This difference in microbiome size also means that HMA sponges have a higher assimilation efficiency of DOM compared to LMA sponges (Bart et al., 2020). LMA sponges, on the other hand, compensate for the decreased size of their microbiome and their ability to utilize DOM as a food source by relying on pumping large volumes of water and filtering more particulate organic material (Hentschel et al., 2006). In HMA sponges, the high abundance of associated microbes can account for up to 35 % to 40 % of the total biomass (Vacelet and Donadey, 1977). This high microbial biomass is crucial for the sponge's nutrition and overall health, as these microbes play essential roles in nutrient cycling and DOM processing within the sponge. Furthermore, bacterial symbionts from HMA sponges possess a wide variety of genes that confer unique biogeochemical attributes not commonly found in other animals (Webster and Thomas, 2016). The ability of sponges to consume DOM can have a ripple effect throughout the food chain since HMA sponges utilize organic matter that is not available to other organisms and transfer it to higher trophic levels (Hanz et al., 2022). In this way, they play an important ecological role as pseudoautotrophic producers and facilitate the indirect transfer of DOM via sponges to higher trophic level predators. Additionally, DOM assimilated into larger organic material by sponges can be excreted as detritus, which can be consumed by other animals in a process known as the sponge loop (De Goeij et al., 2013).

Like phytoplankton, DOM can also bind Hg, but how DOM interacts with Hg depends on several factors, including the source of DOM. Marine DOM enhances phytoplankton MeHg uptake by facilitating active transport through membrane channels (Garcia-Arevalo et al., 2024; Schartup et al., 2015), whereas terrestrial DOM inhibits the uptake of MeHg by biota due to stronger thiol binding (Seelen et al., 2023). DOM also binds inorganic Hg (iHg), influencing its speciation and bioavailability for microbial methylation (Graham et al., 2012). Since sponges can consume DOM, and DOM has different Hg binding patterns from phytoplankton, it raises the question of whether DOM consumption in sponges would consequently have different Hg bioaccumulation patterns compared to phytoplankton consuming benthos.

1.2 Hg in sponges

Studies analyzing iHg and MeHg in sponges found extreme variability in the iHg and MeHg content. Orani et al. (2020) found that in the Mediterranean Sea sponges generally have extremely low MeHg and a low MeHg / Hg ratio of 4 %, while sponges in the intertidal area of the Celtic Sea have very high MeHg concentrations and high MeHg / Hg ratios of between 7 % and 28 %. Recent efforts in sponge identification suggest that of the 4 sponges sampled from Orani et al. (2020) from the Mediterranean Sea, 3 species are classified as LMA sponges; *Acanthella acuta* (Gloeckner et al., 2014), *Cymbaxinella damicornis*, recently reclassified under the genus *Axinella* (Erwin et al., 2015), and *Haliclona fulva* (García-Bonilla et al., 2019), while 1 sponge, *Chondrilla nucula*, is classified as HMA (Thiel et al., 2007). Since sponges can form the majority of the benthic biomass in sponge reefs and are commonly predated upon, their MeHg content likely influences MeHg levels in higher trophic level animals. This raises the question of whether MeHg bioaccumulation in

higher trophic levels in (HMA) sponge dominated systems differs from the bioaccumulation in non-sponge-dominated ecosystems.

The low MeHg content in sponges in the Mediterranean Sea is proposed to be caused by active in vivo MeHg demethylation by Orani et al. (2020). This is because HMA sponges have been found to contain bacterial symbionts that possess the MerA and MerB genes (Santos-Gandelman et al., 2014). The MerA gene transcribes the mercuric reductase protein that converts Hg^{2+} to volatile Hg^0, and merB transcribes for organomercurial lyase, which catalyzes the breakdown of the C-Hg bond through protonolysis and can demethylate toxic MeHg into less toxic iHg (Mathema et al., 2011). However, this does not explain the low concentration of MeHg in LMA sponges nor the high concentration of iHg in both LMA and HMA sponges. An alternative proposal for the low MeHg concentration in HMA sponges is that it is low due to the consumption of DOM. This is suggested in Amptmeijer et al. (2025b), which presents a modeling study examining how the feeding strategy influences iHg and MeHg dynamics. In this model, the MeHg partitioning to DOM, which is based on the MERCY v2.0 model, results in lower MeHg concentration in DOM compared to phytoplankton. This results in DOM consuming suspension feeders, such as sponges, having less MeHg bioaccumulation than filter feeders consuming phytoplankton, zooplankton, and detritus. In that model, the feeding strategy is considered in isolation, and other biological factors that could affect bioaccumulation are not included, such as in vivo demethylation, the long lifespan of sponges, and their low metabolic rate. Additionally, the model is simulated in conditions representing the North Sea, where HMA sponges are not abundant. The model presented in this manuscript expands on the model presented by Amptmeijer et al. (2025b) by creating a more realistic model of sponges. We focus on incorporating the life cycles and feeding behaviors of megabenthos groups to enhance the understanding of iHg and MeHg bioaccumulation in Mediterranean Sea sponges while running the simulation under hydrodynamic and climatological conditions typical of the Western Mediterranean Sea, where both LMA and HMA sponges are common.

Most ecosystems rely on phytoplankton as the base of the food web, meaning that MeHg bioaccumulation can often be estimated from trophic level and phytoplankton MeHg concentrations. Sponge-dominated systems differ in that sponges can efficiently utilize DOM as a food source and exhibit extremely low MeHg concentrations compared to other megabenthos (Orani et al., 2020). This is important because the main predictor of MeHg concentrations in high trophic levels is the MeHg concentration at the base of the food web and the trophic level itself (Wu et al., 2019; Lavoie et al., 2013). Because sponges can form the majority of the benthic biomass in sponge reefs and are commonly predated upon, the MeHg content of sponges is likely directly linked to the MeHg content of higher trophic level animals, although this relationship remains understudied. We therefore hypothesize that the low MeHg concentrations in sponges lead to reduced MeHg bioaccumulation in high trophic level animals inhabiting sponge grounds compared to animals of similar trophic position in other ecosystems.

1.3 The hypotheses

We test the following hypotheses using a modeling approach:

- The low MeHg concentrations in LMA sponges can be attributed to their consumption of DOM, while the even lower levels observed in HMA sponges are likely due to both DOM consumption and active demethylation.
- The elevated iHg concentrations in both LMA and HMA sponges can be explained by their uptake of iHg from DOM.
- Sponges can reduce the MeHg concentration in benthic fish by having a low MeHg concentration and forming the base of the food web

To test these hypotheses, we constructed a model to trace the bioaccumulation of MeHg within the Mediterranean Sea food web in the Bay of Villefranche, a region of notable concern with respect to Hg contamination (Claisse, 1989). This enables us to assess the levels of iHg and MeHg accumulating in LMA sponges and determine if our model can accurately replicate the observed data. The demethylation rate necessary to account for the observed differences between LMA and HMA sponges was then estimated by a sensitivity study in which the model was run with differing MeHg demethylation rates in HMA sponges. Finally, the model was used to assess the differences in MeHg bioaccumulation in fish in a setup with and without sponges to see if sponges influence MeHg bioaccumulation in fish. Given the limited observational data available and that the model is 1D without a vertical component, this study serves as a proof-of-concept to evaluate whether these mechanisms are numerically plausible, but their verification and quantification require empirical validation.

2 Materials and methods

2.1 The model domain – The Bay of Villefranche

The Bay of Villefranche is a natural bay located just west of the French-Italian border, near the French town of Villefranche-sur-Mer. The bay is known for its deep oligotrophic waters, steep underwater topography, rocky inlets, and sandy bottoms. The nearby Villefranche Canyon creates diverse habitats that support a range of benthic communities. The model was run at a 17 m deep location (43°41′53.23″ N, 7°18′57.02″ E) to resemble the depth at which the sponge samples, to which the model is compared, were taken. Monitoring programs within the bay have mainly focused on

planktonic research in coastal waters (Dolan, 2014). Therefore, similar and abundantly available long-term benthic community data from nearby areas of the Gulf of Lyon were used to evaluate our model. In Fig. 1, we show the model domain; where Fig. 1a) depicts the Western Mediterranean Sea, while Fig. 1b) shows the exact modeled location in the Bay of Villefranche. The maps were created in R using Esri WorldImagery.

2.2 The hydrodynamic model - GOTM

The one-dimensional (1D) Generalized Ocean Turbulence Model (GOTM) is used as the hydrodynamic model, which calculates the turbulence of a vertical 1D water column setup by computing the solutions to the 1D version of the transport equation of momentum, salinity, and temperature (Bolding et al., 2021). The model is nudged to observational data sets for temperature and salinity. The setups are designed using the hGOTM tool, which is driven by gridded bathymetry data for water depth (1/240°) (GEBCO Bathymetric Compilation Group, 2020), the ECMWF ERA5 dataset for meteorological data (Wouters et al., 2021), and the World Ocean Atlas for salinity and temperature profiles (Garcia et al., 2019).

2.3 Coupling GOTM to the biogeochemical models using FABM

The MERCY v2.0 model and the ECOSMO E2E model are coupled to the GOTM model using the Framework for Aquatic Biogeochemical Modeling (FABM) (Bruggeman and Bolding, 2014). The biogeochemical models are coded into FABM. The FABM interfaces communicate the state variables between the GOTM model and the biogeochemical models. Physics is modeled with a vertical grid resolution of 0.71 grid cells m^{-1}. The model's state variables are updated every 120 s using the forward Euler method to solve the ordinary differential equation.

2.3.1 Hg cycling and speciation - the MERCY v2.0 model

Hg speciation and cycling are simulated using the MERCY v2.0 model (Bieser et al., 2023). This model represents the major Hg species in marine systems, including elemental Hg (Hg^0), dissolved Hg (Hg^{2+}), monomethylmercury ($MMHg^+$), dimethylmercury (DMHg), and particulate HgS, as well as their partitioning to detritus and dissolved organic matter (DOM).

Within the model framework, Hg^0 and DMHg are treated as volatile species that can evade to the atmosphere. Bioaccumulation is restricted to Hg^{2+} and $MMHg^+$, the only species known to bioaccumulate (Morel et al., 1998), and includes both bioconcentration and biomagnification across trophic levels. For clarity, Hg refers to the sum of all Hg species, MeHg to the sum of $MMHg^+$ and DMHg, and iHg to all non-methylated species. A full list of abbreviations and modeled species is provided in Table 1.

2.3.2 Carbon cycling and ecosystem dynamics - the ECOSMO E2E model

The ecosystem in which Hg bioaccumulates is simulated using an altered version of the ECOSMO E2E model. The original ECOSMO model presented by Daewel and Schrum (2013) is expanded in the ECOSMO E2E model to incorporate higher trophic levels while preserving consistency in lower trophic levels (Daewel et al., 2019). Several adjustments to this model are presented in Amptmeijer et al. (2025a) to make sure that the model, which is originally developed for carbon cycling, is also suitable for bioaccumulation. In this paper, the ECOSMO E2E model is further altered by expanding the megabenthos by splitting it into 6 megabenthos groups separated by their feeding strategies. For every group, a model organism is selected based on which group is parameterized. The megabenthos groups and model organisms are filter feeders (mussel; *Mytilus* sp.), deposit feeders (lugworm; *Arenicula marina*), generalist feeders (brown shrimp; *Crangon crangon*), LMA sponges; (*Mycale hentscheli*), suspension feeders with HMA sponges (*Chondrilla nucula*), benthic predators (shore crab; *Carcinus maenas*), and benthic fish (European plaice; *Pleuronectes platessa*). The benthic fish replaces the pelagic fish that was present in the previous version of the ECOSMO model, to better represent the characteristics of the shallow water in the Bay of Villefranche. The specific species used for this model are not always the main species in these ecosystems, as biological rate measurements are not available for most species. However, we assume that biological rates are representative of broader functional groups and still represent the expected ecosystem functioning.

2.4 Nutrient fluxes in the 1D model

Nutrient cycling is normally dependent on lateral fluxes that are not present in a 1D water column model. To compensate for this, an atmospheric deposition of 0.01 mmol NO_3 d^{-1}, 0.01 mmol NH_4 d^{-1}, 0.5 µmol PO_4 d^{-1}, and 5 µmol SiO_4 d^{-1} (d^{-1} denotes per day) is introduced to compensate for the burial of organic material. This approach of using atmospheric deposition as a tuning parameter follows the methodology applied in the 1D GOTM-ECOSMO-MERCY setups for the North and Baltic Seas used in Amptmeijer et al. (2025a). The deposition values are chosen to produce realistic wintertime nutrient concentrations and support chlorophyll levels in line with observed data. This is further evaluated in the model evaluation section.

2.5 The megabenthos model

The physiological parameters of megabenthos within our model are derived from rates observed in laboratory condi-

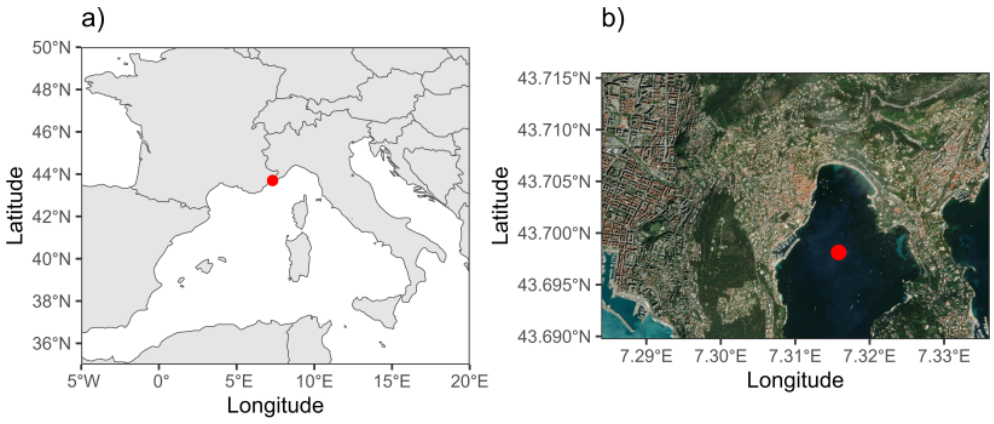

Figure 1. The modeled station is indicated by the red dot. **(a)** Overview map of the western Mediterranean Sea showing the location of the Bay of Villefranche. **(b)** Detailed map of the bay showing the exact sampling location.

Table 1. Definitions of Hg abbreviations.

Abbreviation	Meaning
Hg	Refers to Hg in general
Hg^{2+}	Dissolved Hg (Bioaccumulates)
Hg^{0}	Elemental Hg (Volatile)
$MMHg^{+}$	Monomethylmercury (Bioaccumulates, extremely toxic)
DMHg	Dimethylmercury (Volatile, extremely toxic)
MeHg	$MMHg^{+}$ + DMHg
iHg	Sum of all Hg that is not MeHg
DGM	Dissolved Hg^{0} and DMHg
HMA sponge	High microbial assemblage sponge
LMA sponge	Low microbial assemblage sponge
DOM	Dissolved organic matter
lDOM	Labile dissolved organic matter
sDOM	Semi-labile dissolved organic matter
rDOM	Refractory dissolved organic matter
SPs	sulfated polysaccharides

tions or through field studies. Given the inherent variability present in biological data, definitive rates are not always available and have been inferred from the referenced studies. The deposit feeders, generalist feeders, benthic predators, and benthic fish all feed based on a feeding rate and half saturation. Feeding and respiration rates are presented here as daily rates. Therefore, a feeding or respiration rate of $0.1\,d^{-1}$ would mean that the animal consumes or respires 10 % of its body weight per day. This modeling approach is based on the macrobenthos functional group in the original ECOSMO E2E model (Daewel et al., 2019). The feeding of filter feeders and HMA and LMA sponges is based on their filtration rate within the bottom grid cells of the model. These groups consume a fraction of all food in the bottom grid cell, calculated as their filtration rate [$m^3\,d^{-1}$] divided by the volume of the bottom grid cell [m^3], giving us the uptake [d^{-1}]. There is a maximum consumption rate beyond which a higher concentration of food in the water column will not lead to a higher intake rate. It should be noted that while we estimate the feeding, respiration, and mortality rates of megabenthos based on empirical studies, the modeled animal still represents functional groups. When rates were found in wet weight, a wet weight : dry weight ratio of 1 : 5 was assumed, and when respiration rates were presented by oxygen consumption, a respiratory quotient of 0.85 was assumed to convert oxygen consumption to a respiration rate (Rodil et al., 2019).

The uptake rates of the *deposit feeder* are taken from ex-situ studies performed on a sand-eating lugworm (*Arenicula marina*), whereas this also represents other deposit feeders such as deposit feeding gastropods in the model. The respiration rate based on this study is $0.01\,d^{-1}$, and the mortality rate is $0.0005\,d^{-1}$. The respiration rate is estimated based on the measured oxygen consumption and converted to carbon respiration, assuming a respiratory quotient of 0.85 (Rodil et al., 2019). The mortality rate is based on the observed life

expectancy of 5 years. The grazing rate is 0.12, based on the measured maximum carbon consumption rate (Rijsgard and Banta, 1998; Rodil et al., 2019).

The *filter feeders* in our model are modeled after mussels (*Mytilus* sp.). They are parameterized to have a filtration rate of $9.60 \times 10^{-4}\,m^3\,d^{-1}$, a maximum feeding rate of $0.21\,d^{-1}$, a respiration rate of $0.00867\,d^{-1}$, and a mortality rate of $0.0063\,d^{-1}$ (Koopmans and Wijffels, 2008). The high filtration rate means that filter feeders can grow the fastest of all megabenthos groups in our model when food is abundant, but their high respiration rate means that they are competitively disadvantageous when food is limited.

The model organism for the *generalist feeder* is the brown shrimp (*Crangon crangon*). They eat microzooplankton, mesozooplankton, detritus, and sediment organic carbon. They are estimated to have a lifespan of 3 years, or a mortality rate of $0.0083\,d^{-1}$, and a maximum feeding rate of $0.12\,d^{-1}$ (Perger and Temming, 2012). Regnault (1981) found a respiration rate of per 51 µL $O_2\,h^{-1}$ in a 91 mg^{-1} d.w. shrimp, or $0.55\,mg\,O_2\,g^{-1}$ d.w. This can be translated into a respiration rate of $0.00752\,d^{-1}$ based on a respiratory quotient of 0.85 (Rodil et al., 2019). As a generalist, they thrive in highly variable circumstances where their ability to use different food sources gives them a competitive advantage.

2.5.1 Benthic predator

The benthic predator is the mid-level trophic animal that couples Hg bioaccumulation from the base of the food web to higher trophic levels. As such, this is arguably the functional group that represents the largest number of species in our model. Rates are estimated after the shore crab (*Carcinus maenas*), but the functional group of benthic predators would also include other animals. This is because there is not one animal that feeds on all the included megabenthos groups. Notable predators of HMA sponges are, for example, white seabream (*Diplodus sargus*), the nudibranch *Hypselodoris cantabrica*, and the purple sea urchin (*Paracentrotus lividus*) (Bertolino et al., 2024; da Cruz et al., 2012; Maldonado and Uriz, 1998). The benthic predator is modeled based on laboratory studies of Wallace (1973). They found a feeding rate of $0.065\,d^{-1}$ at 10 °C and $0.13\,d^{-1}$ at 24 °C and observed that the investigated shore crabs were not active below 5 °C. In addition, they found respiration rates between 0.0277 and $0.133\,d^{-1}$. Based on this, we assume that benthic predators below 5 °C do not hunt; above 24 °C they have their optimum grazing rate of $0.13\,d^{-1}$. We used this information to approximate the temperature-dependent respiration ($R_{BP}(T)$) and grazing ($P_{BP}(T)$) rates for the benthic predator as follows:

$$R_{BP}(T) = \begin{cases} 0.00277 & \text{if } T \le 5 \\ 0.00055 \cdot T & \text{if } 5 < T \le 24 \\ 0.0133 & \text{if } T > 24 \end{cases} \quad (1)$$

$$P_{BP}(T) = \begin{cases} 0 & \text{if } T \le 5 \\ 0.0054 \cdot T & \text{if } 5 < T \le 24 \\ 0.13 & \text{if } T > 24 \end{cases} \quad (2)$$

Where T is the temperature in °C. For this benthic predator, we assume a life expectancy of 3 years or a mortality rate of $0.0009\,d^{-1}$.

2.5.2 Benthic fish

The benthic fish is modeled after common species such as the common sole (*Solea solea*), gilthead seabream (*Sparus aurata*), and European flounder (*Platichthys flesus*) which are often found near the seabed among vegetation or sandy substrates. They have a strong temperature-dependent grazing rate and respiration rate. Based on the work by Fonds et al. (1992) on European plaice (*Pleuronectes platessa*) we approximate the temperature-dependent respiration ($R_{BF}(T)$) and grazing ($P_{BF}(T)$) for the benthic fish as follows:

$$R_{BF}(T) = \begin{cases} 0.005 & \text{if } T \le 2 \\ 0.005 + 0.002 \cdot (T-2) & \text{if } 2 < T \le 18 \\ 0.037 & \text{if } T > 18 \end{cases} \quad (3)$$

Max feeding rate

$$P_{BF}(T) = \begin{cases} 0.0135 & \text{if } T \le 2 \\ 0.0135 + 0.0072 \cdot (T-2) & \text{if } 2 < T \le 19 \\ 0.129 & \text{if } T > 18 \end{cases} \quad (4)$$

We assume a lifespan of 2 years, which results in a mortality rate of $0.0037\,d^{-1}$.

A schematic overview of all functional groups of megabenthos and how they are incorporated into the ECOSMO E2E model is shown in Fig. 2.

2.6 Semi-labile DOM

ECOSMO E2E has two forms of pelagic aquatic organic carbon, detritus, and labile DOM (lDOM) (Daewel et al., 2019). Since DOM is a key driver in giving sponges their competitive advantage over other suspension feeders, we also added semi-labile DOM (sDOM). Modeled sDOM does not have a sinking speed; both HMA and LMA sponges can consume it with the same efficiency as lDOM, and bacteria degrade it at the same rate as detritus. When organic material is formed in the model, it is formed as 38 % lDOM, 2 % sDOM, and 60 % detritus. There is an additional rate of sDOM formation from detritus of $0.001\,d^{-1}$. These formation ratios and rates are chosen to have a realistic sDOM value of 0–50 $mgC\,m^{-3}$, based on Lønborg et al. (2024), rather than on established rates of sDOM formation. This is described in more detail in Amptmeijer et al. (2025b).

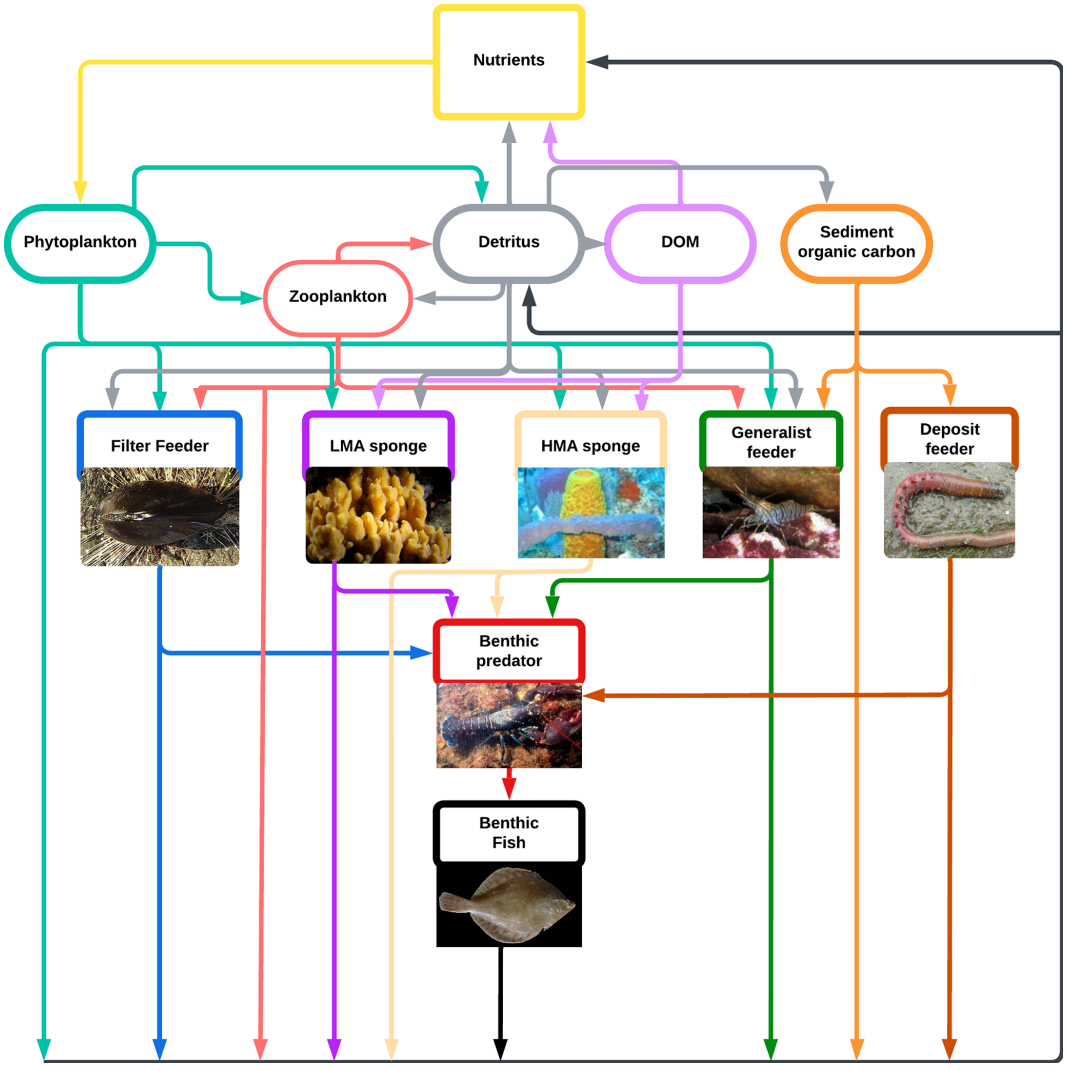

Figure 2. Schematic overview of the implemented megabenthos model. filter feeder: *Mytilus edulis* (photo by Brocken Inaglory, CC BY-SA 3.0, via Wikipedia), HMA sponge: *Aplysina fistularis* (photo by Twilight Zone Expedition Team 2007, NOAA-OE, CC BY 2.0, via Flickr), generalist feeder: *Crangon crangon* (photo by Etrusko25, Public Domain, via Wikipedia), deposit feeder: *Arenicola marina* (photo by Auguste Le Roux, CC BY 3.0, via Wikipedia), benthic predator: *Homarus gammarus* (photo by Bart Braun, Public Domain, via Wikipedia), and benthic fish: *Pleuronectes platessa* (photo by Hans Hillewaert, CC BY-SA 4.0, via Wikipedia). The photo of the LMA sponge was taken by Dr. Eric Wurtz and shared for use in this publication.

2.7 Refractory DOM

In addition to the sDOM added to the model, we also added refractory DOM (rDOM). This DOM is estimated to represent 97 % of the global DOM pool (Baltar et al., 2021; Lønborg et al., 2024). Estimates of rDOM in the Bay of Villefranche are not available, but measurements from a bay on Medes Island estimate the concentration of total DOM at 2.56 gC m^{-3} (Ribes et al., 1999). Since our model has 0–50 mgC m^{-3} sDOM we estimate that an additional 2.5 gC rDOM gC m^{-3} could be present in our modeled domain. Given the uncertainty surrounding the extent to which sponges utilize rDOM when lDOM, sDOM, and detritus are available, and the substantial uncertainty of rDOM's binding to Hg compared to sDOM and lDOM, we run the model simulations both with and without 2.5 gC rDOM m^{-3}. When rDOM is added, it is implemented as a fixed background concentration that is not consumed by bacteria or catabolized into nutrients. This rDOM reacts within the model in two ways. First, HMA sponges can take up rDOM. Since rDOM is represented as constant background concentrations, it is unaffected by sponge uptake. To address this, and considering its low energy value as a food source for sponges, its uptake is limited to 10 % efficiency compared to fresh DOM. Therefore, for HMA sponges, 2.5 gC rDOM m^{-3} corresponds to an equivalent of 0.25 gC m^{-3} lDOM, sDOM, or

detritus in terms of its food availability. The difference in efficiency between the consumption of rDOM and other food sources is not based on a known value, but it is a necessary estimation, since if HMA sponges could feed on rDOM as efficiently as on other food fractions, they would overgrow everything, which is not what is observed in the Mediterranean Sea benthic food web. Because of this, it is used as a tuning parameter to increase the sponge biomass in a somewhat natural way, so we can evaluate the importance of the HMA sponges under different possible circumstances, and can evaluate the influence of sponges on fish MeHg bioaccumulation under a scenario with a high sponge biomass. rDOM is assumed to be mostly organic carbon with no other nutrients. The original ECOSMO E2E model assumes a Redfield Ratio in all consumers, but we deviate from this when HMA sponges consume rDOM to account for the low C : N and C : P ratio in rDOM. When HMA sponges consumes rDOM, the biomass originating from rDOM is tracked, and when they release carbon due to respiration or mortality, the consumed rDOM is not released as labile nutrients for phytoplankton. The same is true when predators and top predators consume HMA sponges directly or indirectly. It is traced how much of the organic carbon originates from rDOM, and when this rDOM-originating organic carbon is released, it is not transferred to dissolved nutrients that are usable by phytoplankton. It is possible that in real life sponges consume rDOM that contains micronutrients, and these nutrients later may be bioavailable, but this is understudied and out of the scope of this model. To summarize, the rDOM approach offers an approximation that allows HMA sponges and their predators to achieve greater biomass without violating the mass conservation principles of the rest of the model, and rDOM does not react directly with any biota, except HMA sponges in the model.

The second way in which rDOM interacts in our model is through partitioning to iHg and MeHg. In the MERCY v2.0 model, the binding partitioning between lDOM and iHg and MeHg is assumed to be based on partitioning coefficient for organic material (the K_d). We use the same partitioning coefficient for lDOM, sDOM, and rDOM. A partitioning coefficient of $\log(K_d) = 6.4$ for iHg and a coefficient of $\log(K_d) = 5.9$ for MeHg is used. This value is the same as is used in Bieser et al. (2023) and is based on Tesán Onrubia et al. (2020).

Our rDOM implementation addresses its absence in the previous version of the ECOSMO E2E model since it is essential for understanding sponge dynamics. The constant concentration reflects rDOM's refractory nature, and the 10 % efficiency assumes lower accessibility compared to fresh organic matter. This enables exploration of an understudied mechanism in Hg cycling. We acknowledge that the rDOM implementation represents a simplified model designed to test whether this mechanism could explain observed patterns or to determine that this is numerically unlikely. The constant concentration and 10 % efficiency assumptions, while necessary for model stability, require empirical validation. This means that this approach can assist our hypothesis-generating model but is not able to generate definitive answers about the importance of rDOM for either sponges or Hg cycling.

2.8 LMA and HMA sponges

LMA and HMA sponges were modeled separately. It must be stated that sponges are an incredibly diverse group, and comprehensive studies analyzing rates in sponges are rare. Because of this, we take the published rates of sponges and evaluate them as well as possible. LMA sponges have a maximum consumption rate of $0.014\,d^{-1}$, a filtration rate of $4.8 \times 10^{-4}\,m^{-3}\,d^{-1}$, and a combined respiration and mortality rate of $0.00257\,d^{-1}$, based on the LMA sponge *Halichondria panicea* (Thomassen and Riisgadrd, 1995). LMA sponges feed on phytoplankton, detritus, lDOM, and sDOM.

To distinguish the LMA and HMA sponges, we make two adjustments. First, the microbiome of HMA sponges gives them the ability to consume rDOM. However, this comes at a cost. HMA sponges are denser and filter water 52 %–94 % slower, due to their investment in maintaining bacterial symbionts (Weisz et al., 2008). However, their uptake efficiency is higher because of the uptake of additional DOM through their symbionts. Because of this, we give HMA sponges a filtration rate of $3.60 \times 10^{-4}\,m^{-3}\,d^{-1}$, which is 25 % lower than the LMA sponges. In our model, HMA sponges feed on detritus, lDOM, sDOM, and rDOM and phytoplankton. When sponges are compared to observations, we assume a carbon to dry weight ratio of 1 : 5, based on Bart et al. (2021). It is worth mentioning that while the 1 : 5 ratio was measured in Atlantic Deep Sea sponges rather than Mediterranean Sea sponges, it originates from the demosponges *Geodia atlantica*, which should resemble the demosponges sampled in Orani et al. (2020).

2.9 Bioaccumulation of Hg and MeHg

The parameters and interactions with respect to bioaccumulation are based on the 1D model presented in Amptmeijer et al. (2025b). Importantly, our model models both the biomagnification and bioconcentration of both iHg and MeHg at every trophic level. In Amptmeijer et al. (2025b) it is shown that this model can accurately model MeHg bioaccumulation at the base of the food web without tuning. The bioconcentration in phytoplankton depends on the size-dependent bioaccumulation and the release rate for both iHg and MeHg. The bioconcentration in all megabenthos is based on the macrobenthos functional group from Amptmeijer et al. (2025a) and they have an uptake rate of $1.68 \times 10^{-5}\,m^3\,mgC^{-1}\,d^{-1}$ and $2.20 \times 10^{-5}\,m^3\,mgC^{-1}\,d^{-1}$ for iHg and MeHg, respectively. All megabenthos have a release rate of $0.04\,d^{-1}$ for iHg while there is no additional release rate for MeHg. Additionally, both MeHg and iHg are released with respiration

and mortality. For biomagnification, an iHg assimilation efficiency (AE) of 0.31 is used and a MeHg AE of 0.95, when biota or detritus is consumed. When sediment is consumed, the AE of iHg is 0.07 and 0.95 for MeHg, based on Dutton and Fisher (2012). When DOM is consumed, the AE is 0.95 for both iHg and MeHg. This is based on the work of Garcia-Arevalo et al. (2024) in phytoplankton, which shows that DOM can play an essential role in facilitating iHg transfer into cells. The assumption is that the DOM molecules are absorbed as a whole, and therefore the iHg associated with this would have a high assimilation efficiency for both iHg and MeHg.

2.10 Scenarios

We suggest that there are 2 pathways leading to HMA sponges having a lower MeHg content than LMA sponges; the consumption of DOM and in vivo demethylation. To assess the relative importance of both pathways we first model the bioaccumulation in HMA sponges under base conditions, where there is no rDOM for the sponges to feed on and the sponges do not demethylate. Afterwards, we simulate sponge bioaccumulation in a scenario where $2.5\,\mathrm{gC\,rDOM\,m^{-3}}$ is present. This allows us to quantify the effect of rDOM consumption on the bioaccumulation of MeHg in HMA sponges. We then perform a sensitivity analysis by varying demethylation rates in HMA sponges to identify the demethylation required to explain the observed MeHg bioaccumulation in LMA and HMA sponges.

Finally, we assess MeHg bioaccumulation in benthic fish by comparing the base case to the scenarios with $2.5\,\mathrm{gC\,rDOM\,m^{-3}}$. This allows us to estimate the potential impact of HMA sponges on MeHg concentrations in fish. We focus on the $2.5\,\mathrm{gC\,rDOM\,m^{-3}}$ scenario because it represents a high HMA sponge biomass resembling a sponge reef. The goal is to evaluate whether this effect is plausible, rather than to quantify its real-world magnitude, as the 1D water column model used here is not suitable for capturing spatial complexity.

2.11 Statistical interpretation of the results

The evaluation of MeHg bioaccumulation in LMA and HMA sponges involves assessing the Mean Percentage Bias (MPB), the equation for which is shown in Table A1 in the Appendix. This metric was chosen because typically, in assessing models, the bias is used, which is the average difference between the model and observations; however, we could not use this due to the uneven amount of data between the model output and observations. Therefore, we first take the mean of the model output and then estimate the percentile bias between the modeled and observed means. This is further supported by performing a Kolmogorov–Smirnov (KS) and Wilcoxon signed-rank (W) tests. Statistical comparisons are used exploratorily to compare model scenarios. The KS test is conducted using the `ks.test()` function, and the Wilcoxon signed-rank test is performed with the `wilcox.test()` function in R (version 4.1.2, "Bird Hippie"). The evaluation considers the D-statistic, the Kolmogorov–Smirnov p-value (KS-p), and the Wilcoxon p-value (W-p). All tests are based on comparisons between the average daily model outputs from the last decade of the simulation and the observations reported by Orani et al. (2020).

The D-statistic measures the maximum deviation between the cumulative distributions of the model and observations, thus measuring the maximum differences in the distribution. A D value below 0.1 suggests very similar distributions, values between 0.1 and 0.5 indicate minor to moderate differences, and a D value greater than 0.5 shows a large difference. The KS-p value calculates whether a significant difference between the modeled and observed distributions exists, while the W-p value estimates the significance of the difference between their medians. P-values below 0.05 for either KS-p or W-p are considered significant.

There is a large difference in sample sizes, with 3652 model data points compared to only 4 (HMA) and 6 (LMA) observations. This imbalance reduces the power of the KS and Wilcoxon tests, making them especially susceptible to false-negative outcomes. This means that high p-values cannot confirm model fit, whereas low p-values (< 0.05) are more reliable indicators of a mismatch between the model and observations.

This limitation is particularly relevant for the Kolmogorov–Smirnov test, as it evaluates the distribution. With only 4 and 6 data points, the observational distribution cannot be robustly defined, but significantly low (< 0.05) p-values still strongly indicate a mismatch between the modeled distribution and the limited observations.

Therefore, these metrics are mainly used to compare which setup performs better relative to other setups and to flag poor-performing configurations. However, they cannot be used to fully determine whether the model simulations are in agreement with observations due to the limited number of observations.

3 Model evaluation

3.1 Evaluation of Nutrient cycling

As mentioned in the methods section, the nutrient deposition is selected to create a realistic phytoplankton community to drive our megabenthos model. In our model, the wintertime nutrient concentrations are $0.12\,\mu\mathrm{mol\,L^{-1}}\,NH_4^+$, $5.0\,\mu\mathrm{mol\,L^{-1}}\,NO_3^-$, $0.3\,\mu\mathrm{mol\,L^{-1}}\,PO_4^{3-}$, and $1.6\,\mu\mathrm{mol\,L^{-1}}\,Si(OH)_4$. These values are on the higher end of observations in the Western Mediterranean Sea but align with elevated nutrient concentrations found in the Gulf of Lion, where surface nitrate and phosphate concentrations reach up to 3.58 ± 1.16 and

0.2–0.3 µmol L^{-1}, respectively . While the modeled silicate concentration is on the lower end of the observed range (1.6–5.8 µmol l^{-1}), based on the World Ocean Atlas 2018, silicate is not typically a limiting factor for phytoplankton growth in the Western Mediterranean, making this value acceptable for our modeling purposes (Belgacem et al., 2021). Based on this, we conclude that the modeled nutrient concentrations are in line with observations and can be used to simulate phytoplankton in our model.

3.2 Evaluation of primary production

We evaluate the modeled chlorophyll *a* concentrations against NASA MODIS-A satellite chlorophyll time series, for the same geographic location (https://oceancolor.gsfc.nasa.gov/, last access: 20 May 2026). The observational chlorophyll time series was sourced from the COPEPOD project (REPHY, 2020). The NASA combined-satellite chlorophyll data presents monthly mean values, allowing for a comprehensive comparison. To evaluate whether the model captures the general chlorophyll a dynamics of the region, we focused on monthly means. Specifically, we averaged modeled chlorophyll values for each calendar month over the last decade of the simulation (e.g., the mean of all Januarys, all Februarys, etc.), and compared these to the corresponding monthly means from the NASA dataset.

While this approach smooths over interannual variability, it offers a way to assess whether the model captures the typical seasonal cycle and magnitude of phytoplankton. Given our focus on bioaccumulation processes, this comparison helps ensure that the modeled phytoplankton concentrations are within a realistic range and appropriate for driving biogeochemical dynamics in the Bay of Villefranche.

The results of the chlorophyll comparison between the model and the observations are shown in Fig. 3a, and the corresponding Taylor diagram is shown in Fig. 3b. The equations from which the metrics are derived are shown in Table A1. The modeled and observed chlorophyll concentrations exhibit a Pearson correlation of 0.59. The root mean square error (RMSE), is 0.127 mg m^{-3}. The maximum observed chlorophyll is 0.54 mg m^{-3} and modeled is 0.55 mg m^{-3}, while the observed mean is 0.31 mg m^{-3} and the modeled mean is 0.28 mg m^{-3}, resulting in a mean bias of -0.028 mg m^{-3}. Overall, the comparison reveals a low bias and relatively high correlation, indicating that the modeled phytoplankton dynamics are consistent with expectations for the Bay of Villefranche and provide a suitable basis for the biogeochemical processes explored in this study.

3.3 Evaluation of the megabenthic biomass

The benthic communities in this area have high specialization and display a patchy distribution, complicating the evaluation of our 1D model. According to Rosenberg et al. (2003), biomass values in the shallow Bay of Lyon vary widely, between 0 and 40 g ash-free dry weight m^{-2}, showing notable regional differences. Despite this, our modeled benthic biomass at 17 m ranges between 3.5 and 5 gC m^{-2}, as shown in Table A2 and visualized in Fig. 4. This means that the biomass in our model is within the observed range. In the Gulf of Lyon, distinct benthic communities dominated by filter feeders (e.g., *Spisula subtruncata*, *Venus ovata*), deposit feeders (*Scoloplos armiger*), and generalist predators (*Nephtys hombergii*) have been identified (Labrune et al., 2007; Fromentin et al., 1997; Rosenberg et al., 2003). Although our 1D model cannot resolve these complex spatial differences, our model does support stable populations of all megabenthic functional groups, making it a reasonable representation of the general benthic community structure in the area.

3.4 Evaluation of Hg and MeHg concentrations

Bioaccumulation starts with the dissolved concentration of the pollutants. Therefore, it is essential to assess that the MERCY v2.0 model generates concentrations of Hg and MeHg that are in line with observations. Our model estimates Hg and MeHg concentrations in the Bay of Villefranche of 0.97 ± 0.087 and 0.018 ± 0.005 pM respectively. Observations in shallow coastal stations in the Gulf of Lion by Cossa et al. (2017) found mean Hg concentrations of 1.52 ± 1.00 pM and MeHg concentrations of 0.026 ± 0.024 pM; however, some MeHg concentrations were below the detection limit, introducing uncertainty. This means that our modeled Hg and MeHg concentrations are well within the observed range and within 1 standard deviation, with a MPB of -36 % for Hg and -31 % for MeHg compared to the observed mean. Based on these results, we conclude that our model reproduces observed Hg and MeHg concentrations in the water, making it suitable for use in our bioaccumulation modeling framework.

3.5 Evaluation of the MeHg bioaccumulation

The biomass and bioaccumulation biota are shown in Table A2. We first discuss the base case, the simulation without rDOM. Then we discuss the differences in the simulation with 2.5 gC rDOM m^{-3} and how this compares to observations. When data were reported in dry weight, we assumed a 1 : 3 dry-weight-to-carbon ratio for plankton and a 1 : 2 ratio for megabenthos and fish to compare our model output in mgC with the bioaccumulation observed in dry-weight measurements. When fish were reported in wet weight, an additional 1 : 5 dry-weight-to-wet-weight ratio was assumed (Menden-Deuer et al., 2000; Sicko-Goad et al., 1984). Overall, the model reproduces the observed ranges and trophic-level trends reported in the literature. MeHg bioaccumulation in phytoplankton is observed at 2.4 ± 0.8 ng Hg gC^{-1} by Tesán-Onrubia et al. (2023), compared to 1.8 ± 4.2 ng Hg gC^{-1} in the model. Zooplankton

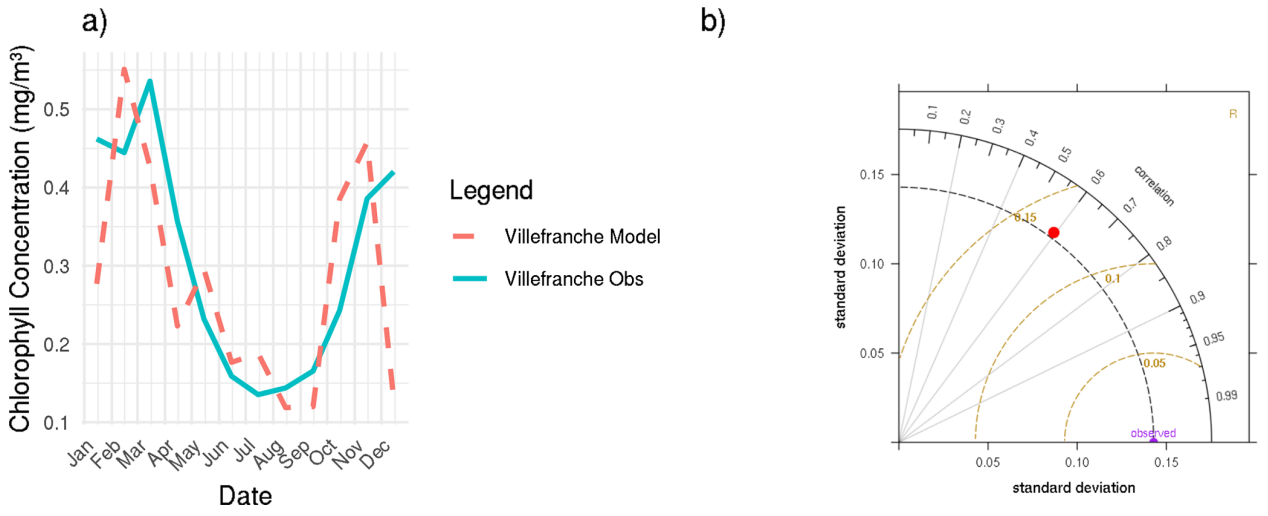

Figure 3. Validation of modeled chlorophyll concentrations. **(a)** Monthly means over the last 10 years from the model and NASA MODIS-A satellite chlorophyll time series. **(b)** Taylor diagram comparing the model and observations, showing a Pearson correlation coefficient of 0.59 and a root mean square error (RMSE) of 0.13 mg m^{-3}, based on monthly means of the 10-year averages.

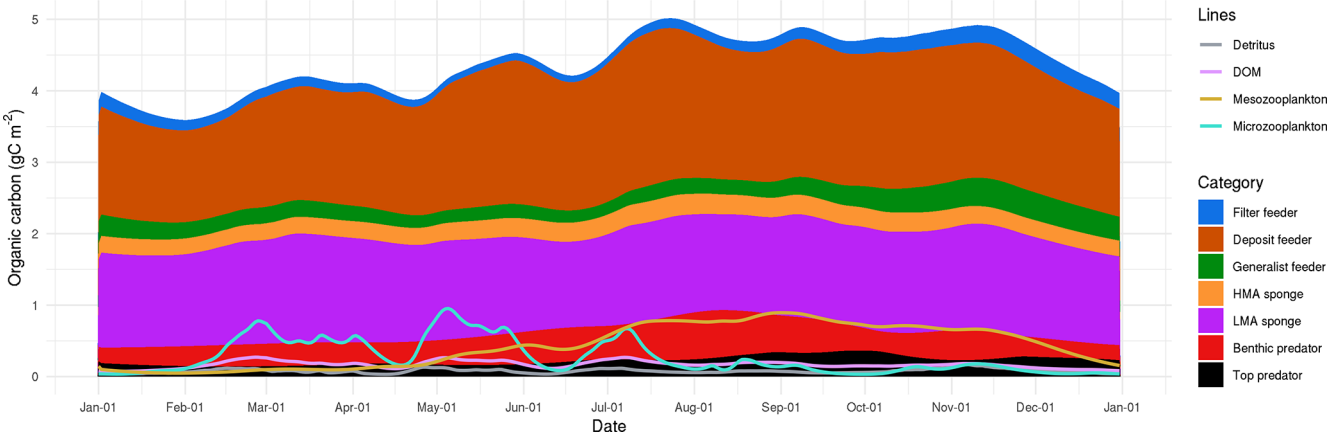

Figure 4. The 10-year average consumer biomass in the base model. Macrobenthos biomass is stacked and pelagic microzooplankton, mesozooplankton detritus and DOM is plotted as lines on top. DOM in this plot is the sum of labile and semi-labile DOM. Macrobenthos biomass is relatively consistent for all groups but dominated by deposit feeders and LMA sponges. Microzooplankton have a spring bloom whereas mesozooplankton are highest in autumn.

observations range from 9–21 ng Hg gC^{-1}, with copepods reaching up to 31 ng Hg gC^{-1} (Buckman et al., 2019) while the model predicts 11.8 ± 4.5 ng Hg gC^{-1} for microzooplankton and 12.6 ± 3.6 ng Hg gC^{-1} for mesozooplankton, so the model is within the observed range.

Filter feeders (oysters and mussels) show observed bioaccumulation of 18–290 ng Hg gC^{-1} along the French coast, and 48–148 ng Hg gC^{-1}, with a mean of 100 ng Hg gC^{-1}, in the Bay of Cannes, which are their closest observations to the Bay of Villefranche (Briant et al., 2017). The model predicts 35 ng Hg gC^{-1}, indicating that the model likely underestimates MeHg bioaccumulation in filter feeders, but the modeled mean still falls within the observed range. Benthic predators have roughly double the MeHg of filter feeders, consistent with biomagnification. Observed MeHg in benthic fish (422 ng Hg gC^{-1}) aligns with mid-trophic Mediterranean species such as common sole (400 ng Hg gC^{-1}) and white seabream (310 ng Hg gC^{-1}). In the 2.5 gC rDOM m^{-3} scenario, low-trophic biota show slightly higher bioaccumulation, likely due to reduced growth dilution. In this scenario, filter feeders are largely outcompeted by sponges. The benthic predator shifts its diet towards HMA sponges, reducing its MeHg to 32 ng Hg gC^{-1} (still approximately three times higher than its diet), and benthic fish MeHg decreases to 205 ng Hg gC^{-1}, consistent with lower-end observations for common sole and closer to species with lower MeHg, such as blackspot seabream or common pandora. Due to the 1D model structure and limited observations, detailed quantita-

tive validation is not possible, but both setups, with and without rDOM, simulate bioaccumulation consistent with observations.

4 Results

4.1 Expected demethylation rate of HMA sponges

Figure 5 shows the bioaccumulation of MeHg in HMA sponges. Without demethylation, the average bioaccumulation of MeHg is higher than the observations in HMA sponges. Having a demethylation rate of $1\,\%\,d^{-1}$ reduces the bioaccumulation of MeHg to $9\,ng\,Hg\,gC^{-1}$, which better aligns it with the average observed MeHg concentration of $13\,ng\,Hg\,gC^{-1}$ in HMA sponges. Furthermore, increasing the demethylation rate to $2.5\,\%\,d^{-1}$ aligns the MeHg content of the HMA sponges with the lowest observations in the HMA sponges. The statistical comparison of the base model and the scenario with 1 % and 2.5 % demethylation per day is shown in Table 2. In the base model, there is a positive MPB for the MeHg content of HMA sponges (+113 %) and the KS-p of <0.001 and W-p of <0.001 show a significant variation between the observed and modeled data, both in their distribution and median values. In the scenario where HMA sponges have 1 % demethylation, the HMA sponges have a smaller negative bias (−30 %) while the D statistic of 0.48 shows a minor difference in the distribution of the modeled and observed bioaccumulation, while the KS-p of 0.309 shows that this difference is not statistically significant. Additionally, the W-p of 0.76 shows that there is also no statistically significant difference between the observed and modeled median MeHg bioaccumulation. In the 2.5 % demethylation per day scenario, the KS-p values (0.023) show no significant difference, while W-p (0.003) value does at the 95 % confidence internval. However, both values are considerably lower compared to the $1\,\%\,d^{-1}$ scenario. These reduced p-values, combined with the high D value of 0.75 and an increased negative MPB of 65 % show that the 2.5 % demethylation per day underestimates the MeHg content of HMA sponges and has lower agreement with the observations than the scenario with 1 % demethylation per day. Under our parameterization assumptions, the model suggests that demethylation rates of $1\,\%\,d^{-1}$ provide reasonable agreement with observations, though this depends critically on uncertain uptake parameters.

4.2 Low MeHg due to DOM consumption in HMA sponges

We investigate the hypothesis that HMA sponges can have low MeHg due to their reliance on DOM as food. To investigate this, we ran the model with $2.5\,gC\,rDOM\,m^{-3}$, which could be consumed by HMA sponges. For HMA sponges, there is no significant discrepancy between the observed and modeled distributions, as signified by a KS-p value of 0.77. Additionally, the D-statistic of 0.33 indicates a moderate similarity between the modeled and observed distributions. The MPB of −2 % along with a W-p value of 0.87 indicates a small bias in the mean, and no significant difference between the modeled and observed median. To summarize, in the scenario with $2.5\,gC\,rDOM\,m^{-3}$ there is no significant difference in either the median or the distribution of MeHg bioaccumulation in HMA sponges. Since the consumption of rDOM alone accounts for the low MeHg levels in HMA sponges, the model was not rerun with a demethylation rate and $2.5\,gC\,m^{-3}$, as this was unnecessary to explain the observed low MeHg concentrations in HMA sponges.

4.3 Low MeHg bioaccumulation in fish due to rDOM consumption in HMA sponges

In our model, consumption of rDOM can influence MeHg bioaccumulation in three ways. First, in our current parameterization, rDOM binds dissolved MeHg, with the same strength as lDOM and sDOM. If we include rDOM, the MeHg concentration per DOM can be reduced due to biomass dilution. This will result in lower concentration of MeHg in suspension feeders consuming DOM, and consequently in predators consuming these suspension feeder. Secondly, the consumption of rDOM by HMA sponges allows the consumption of carbon that is otherwise not bioavailable. This increases the biomass of HMA sponges, and consequently, it increases the biomass of the benthic predator and benthic fish. The shift in biomass causes a shift in the diet of the benthic predator; in the base model, the majority of their diet would consist of deposit feeders and LMA sponges, whereas in the $2.5\,gC\,rDOM\,m^{-3}$ setup, their diet would mostly consist of HMA sponges followed by deposit feeders. Since HMA sponges have an extremely low MeHg concentration, this results in low MeHg in benthic predators and, consequently, in benthic fish. The concentration of MeHg in benthic fish is $422\,ng\,Hg\,g^{-1}$ in the base model and only $205\,ng\,Hg\,g^{-1}$ in the setup with $2.5\,gC\,rDOM\,m^{-3}$. If we run the model with $2.5\,gC\,rDOM\,m^{-3}$, but without HMA sponges, the bioaccumulation of MeHg in fish is $437\,ng\,Hg\,mgC^{-1}$, so comparable to the base case. This means that the HMA sponges in this setup reduce the MeHg content of the fish by 53 %. This effect is not present in the base model, nor in the setup with 1 % demethylation per day, which can be explained by the low biomass of HMA sponges in the base setup compared to the $2.5\,gC\,rDOM\,m^{-3}$ setup. This shows that the 53 % reduction is an upper bound of the reduction that can be expected in benthic fish in ecosystems that are dominated by HMA sponges at the base of the food web compared to ecosystems without sponges.

4.4 The iHg content of sponges

Sponges are observed to have an extremely high iHg content. Orani et al. (2020) observed a mean iHg content of 1523

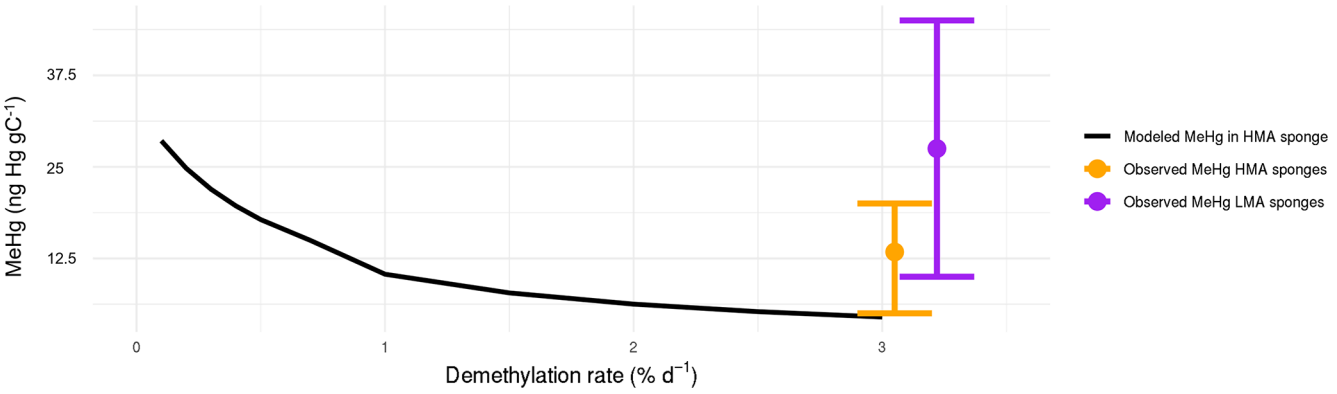

Figure 5. The modeled mean MeHg concentration in HMA sponges with different demethylation rates. Without demethylation, MeHg levels in HMA sponges align with those observed in LMA sponges, as indicated by the purple sidebar. A demethylation rate of 2.5 % d^{-1} reproduces the minimum observed MeHg concentration in modeled HMA sponges, while a rate of 0.5 % d^{-1} reproduces the maximum, as shown by the orange sidebar. A demethylation rate of 1 % d^{-1} in HMA sponges provides the best agreement with the observed mean when rounded down to the nearest 0.5 %.

Table 2. Observed and modeled bioaccumulation of MeHg in LMA and HMA sponges The mean, minimum, and maximum observed and modeled values are shown. Bioaccumulation values are shown in ng Hg mgC^{-1}. For the model scenarios, the mean percentile bias (MPB), the Kolmogorov–Smirnov p-values (KS-p) and D-statistic (D) are shown, as well as the Wilcoxon p-value (W-p). A * marks a significant difference at the 95 % confidence level between the model and observations. In the 2.5 gC rDOM the LMA sponges have no stable population as they are outcompeted by HMA sponges and they are thus omitted from this scenario.

	LMA							HMA						
	Mean	MPB (%)	Min	Max	KS-p	D	W-p	Mean	MPB (%)	Min	Max	KS-p	D	W-p
Observations	31	–	10	45	–	–	–	13	–	5	20	–	–	–
Base model	27	−14	18	71	0.093	0.468	0.215	29	113	22	52	<0.001*	1.000	<0.001*
2.5 gC rDOM	–	–	–	–	–	–	–	13	−2	12	18	0.770	0.332	0.867
1 % Demethylation	27	−14	18	72	0.081	0.479	0.205	9	−30	7	30	0.309	0.483	0.758
2.5 % Demethylation	27	−15	18	71	0.079	0.481	0.203	5	−65	3	16	0.023	0.747	0.003*

* indicates significant deviations between the model and observations at the 95 % confidence interval.

and 696 ng Hg mgC^{-1} in HMA and LMA sponges, respectively, assuming a carbon to dry weight ratio of 1 : 5. Even assuming an AE of 0.95 iHg when DOM is consumed, our modeled iHg bioaccumulation is still an order of magnitude lower than observations. Although fully understanding this is out of the scope of the model, we reproduced the observed concentrations only when the turnover and release rate of iHg in LMA and HMA sponges was completely removed. Under these circumstances, we obtained a bioaccumulation of 1448 and 592 ng Hg mgC^{-1}, or a MPB of 5 % and 15 % in HMA and LMA sponges.

4.5 The maximum and minimum demethylation rates

Since we can replicate the low MeHg content of HMA sponges in the 2.5 gC rDOM scenario, we conclude that in vivo MeHg demethylation is not necessary to explain the observed iHg and MeHg content of HMA sponges. However, the bioconcentration rates of iHg and MeHg in HMA sponges in the model are highly uncertain. If the actual uptake rates are higher, a higher demethylation rate would be required to reproduce the observed values. To estimate an upper bound for the demethylation rate, we assume uptake rates sufficient to reproduce the observed high iHg concentrations in LMA and HMA sponges.

This is achieved by simulating a tenfold increase in LMA sponge uptake rates and a twentyfold increase for HMA sponges in the base case scenario. The resulting uptake rates are 1.68×10^{-4} and 3.35×10^{-4} m^3 mgC d^{-1} for iHg in LMA and HMA sponges, respectively, and 2.20×10^{-4} and 4.41×10^{-4} m^3 mgC d^{-1} for MeHg. Modeled iHg and MeHg concentrations under these conditions are shown in Table 3. Under these circumstances, a demethylation rate of 13 % d^{-1} in HMA sponges gives the best agreement with observations. The demethylation required to reproduce the low MeHg concentrations, therefore, represents a loosely constrained upper bound of the maximum expected demethylation rate.

Table 3. Observed and modeled concentrations of iHg and MeHg in LMA and HMA sponges. The High Uptake (HU) models has uptake rates of 1.68×10^{-4} and 3.35×10^{-4} m^3 $mgC\,d^{-1}$ for iHg in LMA and HMA sponges, respectively, and uptake rates of 2.20×10^{-4} and 4.41×10^{-4} m^3 $mgC\,d^{-1}$ for MeHg in LMA and HMA sponges respectively. In the low Release Rate (LR) model the release rate of iHg is reduced and this is equal to the respiration rate. In the LR model the earlier estimated 1 % d^{-1} in vivo demethylation rate is used while in the HU model the in vivo demethylation rate required to reproduce observels MeHg levels is estimated to be 13 % d^{-1}. Additonally the mean percent bias (MPB) between the modeled and observed concentration is shown. All bioaccumulation values are in ng Hg mgC^{-1}.

	iHg					MeHg				
	Observed	Model (HU)	MPB (%)	Model (LR)	MPB (%)	Observed	Model (HU)	MPB (%)	Model (LR)	MPB (%)
LMA	696	624	−10	556	−20	31	107	245	30	−3
HMA	1523	1415	−7	1397	−8	13	13	0	10	−23

4.6 The high iHg of LMA and HMA sponges.

An additional method for the model to reproduce the high iHg content of sponges is to reduce the release rate. As shown in Table 3, the model also reproduces the high iHg content of both LMA and HMA if we assume that iHg is strongly retained in sponges and is only released at a rate equal to the respiration rate of sponges. This model is referred to as the low release rate model (LR). In this parameterization, there is no additional release rate of iHg in sponges, and iHg is only released with the metabolic rate. This parameterization can reproduce both the iHg and MeHg bioaccumulation in both LMA and HMA sponges with an MPB of 30 % or lower.

4.7 Sensitivity of the results to the rDOM implementation

As discussed in the Methods section, the uptake of rDOM and its efficiency are poorly understood, and we consequently used this parameter for model tuning. In the 2.5 gC rDOM m^{-3} scenario, we assumed an rDOM uptake efficiency of 0.1. To analyze how rDOM consumption and sponges influence MeHg bioaccumulation in benthic fish, we run the model with rDOM uptake efficiencies of 1, 1/5, 1/10, 1/15, 1/30, 1/75 and 1/100. The results are shown in Fig. 6. Figure 6a shows that increasing the efficiency of uptake of rDOM leads to an increase in the biomass fraction of sponges, while Fig. 6b shows that HMA sponges comprise a larger fraction of benthic biomass. At 10 gC m^{-2}, further sponge growth becomes limited in our model due to the assumed substrate limitation. As a result, the fraction of benthic biomass composed of HMA sponges increases rapidly until, at an uptake efficiency of approximately 0.25, sponges represent about 70 %–80 % of the benthic biomass. Further increases in uptake efficiency of up to 1 do not lead to additional increases in the HMA sponge fraction. Figure 6b also shows that as the fraction of benthic biomass composed of HMA sponges increases, the bioaccumulation of MeHg in benthic fish decreases. A visual clustering is observed once sponges exceed approximately 50 % of benthic biomass, suggesting a potential saturation effect by which sponges dominate predator diets. However, this pattern is likely influenced by model structure and feeding parameterisations and may not reflect a general ecological mechanism, as natural systems typically include multiple specialized predators rather than a single generalist consumer.

5 Discussion

A summary of the results is shown in Fig. 7. Figure 7a shows the bioaccumulation of iHg and MeHg in megabenthic groups from observations and different model scenarios. Here we see that the model can produce the observed MeHg concentration in both LMA and HMA sponges. Additionally, it shows that if we assume a reduced iHg release rate of sponges (the LR model), the model can replicate the high iHg and low MeHg concentrations in both LMA and HMA sponges. Figure 7b shows the MeHg bioaccumulation in predators and benthic fish in different modeled scenarios and demonstrates notably lower concentrations of MeHg in both the predator and the benthic fish in the scenario where sponges form the base of the benthic food web. We tested several different scenarios for the bioaccumulation of iHg and MeHg in sponges; here we discuss the differences between these scenarios and how the results of this study can help us better understand the bioaccumulation of Hg in sponges.

5.1 Mechanistic explanation for the special role of DOM in iHg and MeHg bioaccumulation

The difference in bioaccumulation of iHg and MeHg highlights Hg as a unique pollutant. Certain biological pathways, such as the direct absorption of MeHg via membrane channels in phytoplankton, enable highly efficient MeHg bioaccumulation. As a result, MeHg concentrations in biota can exceed iHg concentrations, even in primary producers, despite the fact that dissolved iHg is generally more abundant than MeHg. In DOM, which consists primarily of dead organic particles, these preferential uptake pathways are absent, and DOM binds iHg and MeHg only through scavenging. The composition of DOM strongly influences its binding capacity: thiol-rich fractions of terrestrial DOM efficiently

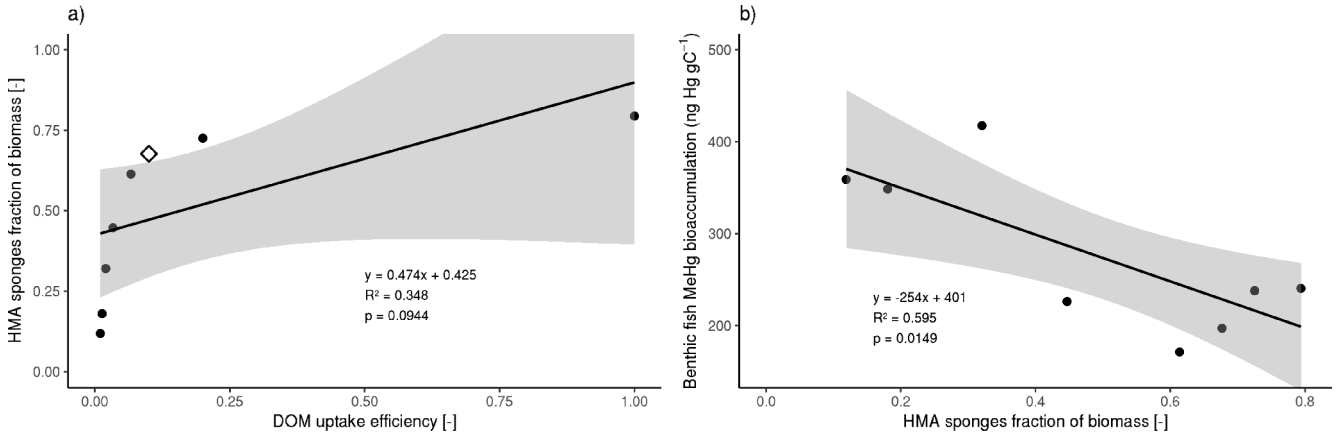

Figure 6. Sensitivity of the model results to the feeding efficiency of HMA sponges on rDOM. Panel **(a)** shows that as the feeding efficiency of rDOM increases, the fraction of HMA sponges among the primary benthic consumers (sponges, filter feeders, deposit feeders, and generalist feeders) also increases. The 0.10 rDOM uptake efficiency that we used in the model is marked as the larger point. Even with the relatively low efficiency of 0.10, as used in the model, HMA sponges remain a major component of the primary benthic consumer biomass. Panel **(b)** illustrates how this increase in the fraction of HMA sponges in the benthic community leads to a decrease in the bioaccumulation of MeHg in fish.

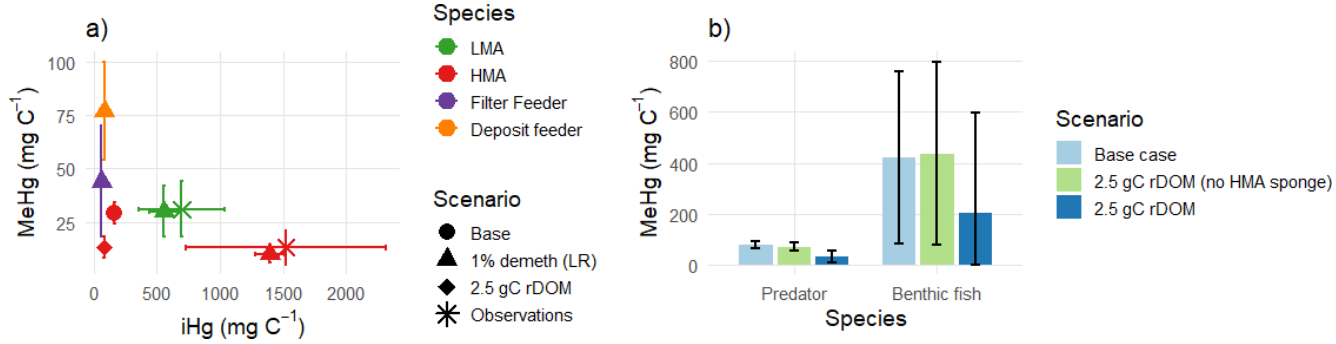

Figure 7. Summary of key results. Panel **(a)** shows the modeled bioaccumulation of iHg and MeHg in megabenthos compared with observed bioaccumulation in LMA and HMA sponges, where triangles indicate model values and circles indicate observations. The scenario with a demethylation rate of 1 % d^{-1} and reduced Hg release shows strong agreement with the observed sponges. Panel **(b)** shows the modeled bioaccumulation of MeHg in predators and benthic fish, with concentrations in fish (blue) reduced by 53 % in the scenario with 2.5 gC rDOM m^{-3} compared to the same simulation without sponges.

bind to MeHg (Seelen et al., 2023), while marine DOM fractions show a higher affinity for iHg (Tesán Onrubia et al., 2020), which underpins the partitioning behavior used in the MERCY v2.0 model (Bieser et al., 2023).

The lack of efficient MeHg uptake mechanisms, combined with low dissolved MeHg concentrations, results in low MeHg bound to DOM in our model, while iHg is higher due to the efficient scavenging of iHg by DOM and the higher dissolved concentration of iHg compared to MeHg. Consequently, when HMA sponges feed on DOM, they accumulate very low MeHg concentrations, whereas the efficient partitioning of iHg to DOM results in elevated iHg levels, even though iHg is not typically transferred via diet very efficiently.

5.2 With or without rDOM; what is the most realistic scenario

As mentioned in the model development segment, an rDOM concentration of 2.5 mgC m^{-3} is observed. However, as the name suggests, this rDOM is refractory and generally unresponsive. This raises the question as to what degree it should be incorporated in the model. There are 2 key questions;

- To what degree do sponges feed on rDOM compared to lDOM and sDOM
- Does Hg bind with equal preference to rDOM, sDOM and lDOM, and is this different for iHg and MeHg.

An argument for focusing solely on lDOM and sDOM can be made based on the work by Seelen et al. (2023). They

show that the thiol content of DOM is lower in marine environments than in rivers and that DOM of terrestrial origin has a stronger affinity to bind MeHg as it is richer in thiol groups. If terrestrial DOM that is non-refractory has a considerably higher affinity to bind MeHg, it is likely that this transfers MeHg to sponges upon consumption. If this is the case, having lDOM and sDOM in our model to bind and transfer MeHg, while excluding rDOM, might replicate real-world circumstances where rDOM does not bind Hg efficiently, but labile fractions of DOM dominate MeHg binding and transfer.

Additionally, while it is currently understood that both HMA and LMA sponges can consume DOM, including rDOM, the degree to which they do this is poorly understood. In shallow Mediterranean Sea water, other food sources are available. Because of this, HMA sponges might predominantly feed on the more labile fractions of DOM, and rDOM could play a minor or insignificant role in both carbon cycling and MeHg bioaccumulation.

Arguments in favor of including rDOM are that we know it is present in large concentrations and there is only limited evidence to suggest it does not play a major role in both Hg and carbon cycling. This is also supported by our model. Our model shows good agreement (% MPB $= -2$ %) with no significant difference (ks-$P > 0.77$) between the modeled and observed MeHg concentrations in HMA sponges when we incorporate rDOM in the model.

Additionally, it is established knowledge that DOM plays an important role in Hg bioaccumulation, as demonstrated by Schartup et al. (2015), and that different DOM fractions can affect Hg bioaccumulation in distinct ways, as shown by Seelen et al. (2023). Therefore, improving the representation of DOM and detritus cycling, particularly by including distinct fractions such as rDOM, represents a logical step forward to increase Hg cycling and bioaccumulation models, even in models that do not incorporate HMA sponges.

To improve the model in this regard, more empirical data are needed to link rDOM to concentrations and composition to bioaccumulation. Improved knowledge of which fractions of DOM are consumed by LMA and HMA sponges and to what degree, coupled with a better understanding of the MeHg binding strength of this DOM fraction, could greatly enhance our understanding of what drives these low MeHg concentrations in HMA sponges.

5.3 The important role of HMA sponges in lowering MeHg content of fish

While demethylation and DOM consumption can both play a role in causing the low MeHg content of sponges, especially HMA sponges, they certainly have an extremely low MeHg content. In addition, HMA sponges can have large biomass and be the main part of low-trophic-level biomass. Our model shows that this can dramatically reduce the MeHg content of higher trophic level benthic fish; in our model, this is a reduction of 53 %. This percentage is, of course, highly dependent on the MeHg concentration of sponges, the MeHg concentration of other megabenthos, and the degree to which sponges are consumed. While the role of sponges in the ecosystem is understudied, it is clear that sponges are both directly and indirectly consumed by important commercial species of fish. The 53 % reduction in MeHg bioaccumulation of fish represents a potential quantification of this effect under extremely high HMA sponge biomass scenarios, while assuming HMA sponges are a critical link in the food chain. These conditions represent an idealized scenario for this effect, which means that it represents an upper bound estimate that requires further study under natural conditions to be quantified.

5.4 The iHg content of sponges

The model mainly focuses on explaining the low MeHg content of the sponges and the observed difference between LMA and HMA sponges. However, investigating the unusually high iHg content of HMA sponges is an essential part of the Hg sponge biochemistry and should be taken into account. We demonstrate that we can explain both the iHg and MeHg concentrations found in HMA sponges by assuming an iHg and MeHg uptake rate of $3.35 \times 10^{-4}\,\mathrm{m^3\,mgC\,d^{-1}}$ for iHg and $4.41 \times 10^{-4}\,\mathrm{m^3\,mgC\,d^{-1}}$ for MeHg. The issue with this parameterization is that we can offer no explanation for the low MeHg content of LMA sponges. An additional way we can reproduce the observed iHg content of sponges is sponge retain Hg stronger than other macrobenthos. We can reproduce the high iHg content of both HMA and LMA sponges if we assume that the release rate of iHg is equal to the carbon respiration rate of the sponge, which is much lower than what has been observed for other animals such as small crustaceans and bivalves (Tsui and Wang, 2004; Pan and Wang, 2011). While this is speculative at the moment, a potential explanation can be found in the unique structure of sponges. A study on the glass sponge *Euplectella aspergillum* found that they have elevated Hg levels in the spicules. *C. nucula* is a demosponge, not a glass sponge, but it still has glass spicules. But a similar buildup of iHg in structural components of the sponge might be happening in other components of the sponge. Demosponges rely on a protein called spongin and sulfated polysaccharides (SPs) to bind the sponge together. A possible explanation for the reduced release rate of iHg in sponges could be that iHg remains bound to the SPs in sponges.

We propose this for three reasons.

- SPs in *C. nucula* have a very high sulfate to sugar ratio of 1 : 5 (Vilanova et al., 2007).
- SPs with high sulfate content have been found to bind $50\,\mathrm{mg\,Hg\,g^{-1}}$ SPs (Cruz et al., 2017).
- Sponges contain up to 3 % SPs, providing abundant bindings sites for iHg (Esteves et al., 2011).

Combining these observations, we can estimate that sponges with 3 % dry weight SPs would be able to bind 1500 ng Hg mg^{-1} dry weight, or 7500 ng Hg mgC^{-1} assuming a 1 : 5 carbon to weight dry weight ratio. This is higher than observed and shows that the SPs in *C. nucula* would be able to store the observed Hg concentrations. Note that this is a rough estimation and, for example, the iHg binding data of the SPs are based on bacterially produced linear SPs rather than branched SPs produced by demosponges. It does, however, indicate that the high SPs content of the sponge could explain its high iHg content. Given that our model predicts elevated iHg concentrations in sponges due to DOM consumption, but it cannot fully reproduce the observed iHg levels, it seems the high iHg content in sponges results from a combination of both drivers.

5.5 Low MeHg in HMA sponges; Demethylation, DOM consumption or both

Since our model can reproduce MeHg concentrations without demethylation in both HMA and LMA sponges, it shows that demethylation may not be necessary to describe the observed patterns. This does not mean that demethylation cannot play a role, but since LMA sponges do not contain large amounts of sulfate-reducing bacteria that can demethylate MeHg, a compelling argument can be made based on our model that the low MeHg concentration in LMA sponges is caused by the consumption of DOM and detritus, which make up a substantial part of their diet. The even lower MeHg content of HMA sponges can then be explained by an increased dependence on DOM by HMA sponges, in vivo MeHg demethylation, or a combination of both.

The expected demethylation rate is linked to the uptake rate of MeHg, which is uncertain. Because of this, we see two potential pathways that lead to the observed bioaccumulation of iHg and MeHg in LMA and HMA sponges.

The scenario with no in vivo MeHg demethylation, as is explored in the 2.5 gC rDOM scenario, and low in vivo MeHg demethylation, as is explored in the 1 % demethylation scenario, can both reproduce the observed MeHg concentration in LMA and HMA sponges, but lack a full explanation for the elevated iHg concentration in sponges. Because of this, we conclude that both no or low in vivo MeHg demethylation in HMA sponges is possible, and we supplement this paper with a proposed explanation on why sponges could have high iHg based on their chemical composition.

Consequently, we consider it most likely that the high iHg content of sponges results from a reduced release rate of iHg, possible due to iHg accumulation on SPs or spongin. The low MeHg levels in LMA sponges are attributed to the consumption of DOM, while the reduced MeHg levels in HMA sponges arise from DOM consumption, possibly accompanied by an in vivo demethylation rate of 1 %.

5.6 Limitations of the rDOM implementation

A major simplification in our model lies in the implementation of rDOM. In our setup, rDOM serves as a proxy for organic material that can be consumed by HMA sponges but is not dissimilated by non-sponge-associated microbes on timescales relevant to our model. This approach is particularly suited to a 1D configuration, where a constant flow of rDOM can be assumed throughout the system. The current implementation was chosen to ensure consistency in nutrient availability for phytoplankton growth, to preserve mass balance across the model, and to enable HMA sponges to use rDOM for growth; as such, it serves as a useful proof of concept to explore whether rDOM could play a meaningful role in ecosystem functioning. However, this implementation is limited in scope. In a 3D model or in stratified water columns where vertical mixing is reduced, rDOM transport may significantly influence the distribution and cycling of Hg. Furthermore, potential effects of rDOM, such as its role in light attenuation, are not incorporated in the model. To fully assess the role of rDOM in both HMA sponge ecology and Hg biogeochemistry, cycling, and bioaccumulation, a more realistic representation will be necessary.

5.7 Broader limitations and future research needs

Beyond the limitations of the rDOM implementation, several major limitations affect the model. The most important is the low data availability. Our conclusions rely on a single study of MeHg and iHg bioaccumulation in Mediterranean sponges, with small sample sizes ($n = 4$ for HMA and $n = 6$ for LMA sponges). While the model–data comparison allows identification of clear mismatches between the model and observations, the limited number of observations prevents reliable validation of simulated Hg bioaccumulation patterns. Therefore, the agreement between model simulations and observations should be interpreted with care.

In addition, key processes remain poorly mechanistically understood. The mechanisms and rates of (r)DOM consumption by sponges, the role of sponges in ecosystem-level Hg bioaccumulation, and the functional differences between LMA and HMA sponges are not fully understood. These knowledge gaps limit process-based parameterization and increase structural uncertainty in the model.

Because of this, targeted empirical studies on Hg bioaccumulation in sponges, including controlled experiments focused on the bioaccumulation pathways that were flagged as potentially significant in this model, such as the role of the uptake of DOM by sponges on Hg bioaccumulation and the consumption and trophic transfer of Hg of sponges by predators, could substantially improve model development by enabling more robust validation.

We focus on qualitative model insights rather than extensive sensitivity analyses. While all parameters carry uncertainty, our primary objective is to demonstrate that the pro-

posed mechanisms are quantitatively plausible alternatives to the demethylation hypothesis proposed by Orani et al. (2020). Comprehensive sensitivity analyses would confirm parameter uncertainty without providing additional mechanistic insights. Rather, we demonstrate that our base parameterization can reproduce the observed bioaccumulation of MeHg in both LMA and HMA sponges linked to the consumption of DOM and rDOM, which shows that DOM consumption by LMA sponges and rDOM consumption by HMA sponges could reproduce the observed patterns.

Based on the literature, we assume that sponges form an integral part of the food chain, leading to our hypothesis that sponges might reduce MeHg bioaccumulation in animals above them in the food web, including commercially important fish species. The predicted 53 % reduction in benthic fish MeHg concentrations represents a hypothesis-generating finding that demonstrates the potential magnitude of sponge-mediated effects. This should be interpreted as a loosely constrained upper bound estimate, given our generous parameterization of HMA sponge biomass and role in the food chain. The actual magnitude would depend on local sponge abundance, community structure, and food web dynamics. Both our mechanistic understanding of food web dynamics in the Bay of Villefranche and the role of sponges in them, and the dynamics between sponges and iHg should be validated with empirical studies before this estimation can be meaningfully constrained using sensitivity studies.

5.8 A potential role of sponges in bioremediation

Sponges are unique in their ability to bioaccumulate Hg, as they both have extremely high levels of iHg while maintaining very low levels of MeHg. This characteristic makes them a prime candidate for bioremediation studies. If the model is accurate for sponge grounds, they could be advantageous for Hg remediation. On the one hand, in Hg-polluted regions, sponges could bioaccumulate the less toxic iHg, which could then be extracted for bioremediation, with a diminished risk of MeHg since the majority of the Hg remains in its unmethylated form. Furthermore, the low MeHg content in HMA sponges means that organisms feeding on them would accumulate less MeHg, ultimately resulting in lower MeHg levels in higher trophic levels, as demonstrated in our model. These findings suggest that actively managing sponge grounds could both mitigate MeHg accumulation in fish and provide a sustainable method for extracting Hg from the marine environment.

6 Evaluate the hypotheses

We accept the hypothesis that *the consumption of DOM can explain the low MeHg content of LMA sponges, while a combination of consumption of DOM and demethylation explains the even lower concentration in HMA sponges*. We expand this by showing that while demethylation can play a role, DOM consumption can explain both the low MeHg concentration in LMA sponges, while the even lower concentration in HMA sponges can be explained by rDOM consumption or a demethylation rate of 1 % d^{-1}.

We reject the hypothesis that *the consumption of DOM can explain the high iHg values of LMA and HMA sponges*. Even with an assimilation efficiency of 0.95 for iHg when DOM was consumed, our modeled iHg bioaccumulation was still an order of magnitude lower than observed. We demonstrate that the consumption of DOM can increase the iHg content in sponges, but to reproduce the iHg bioaccumulation, we need to assume that iHg is only released with respiration and not through an additional turnover or respiration rate, or that sponges have an elevated iHg uptake rate. We expand by providing an explanation of how we think that the binding of iHg to SPs in sponges can reduce the iHg from sponges.

We accept the final hypothesis that *sponges can lower the concentration of MeHg in fish*. We supplement this by showing a reduction of 53 % in our model.

7 Mechanistic summary of the model results

The model demonstrates two main conclusions, but it is important to summarize the proposed mechanisms. These mechanisms are visualized in Fig. 8. First, measurements show that sponges have elevated iHg and low MeHg levels, particularly HMA sponges. Both HMA and LMA sponges can consume DOM, although HMA sponges do so more efficiently. Additionally, measurements indicate that DOM contains relatively more iHg and less MeHg compared to phytoplankton. Consequently, our model suggests that an ecosystem with (HMA) sponges at its base can rely partially on DOM consumption rather than phytoplankton, resulting in elevated iHg and reduced MeHg at the base of the food web.

Second, we propose that, because the biomagnification factor of iHg is very low, while it is extremely high for MeHg, a sponge dominated ecosystem with significantly lower MeHg concentrations at the base would show a significant reduction in MeHg in higher trophic levels. Although the 1D model used in this study is not suitable for reliable quantification of this effect, it is mechanistically intuitive that an ecosystem with filter feeders at its base with MeHg levels between 48 and 148 ng Hg gC^{-1} would lead to higher bioaccumulation in upper trophic levels than a system dominated by HMA sponges with low MeHg concentrations of around 13 ng Hg gC^{-1}.

8 Summary and Conclusion

In this study, we modeled the benthic ecosystem of the Bay of Villefranche using the 1D GOTM-ECOSMO-MERCY coupled system. The simulated chlorophyll concentrations align with the NASA MODIS-A satellite time series. Pelagic iHg

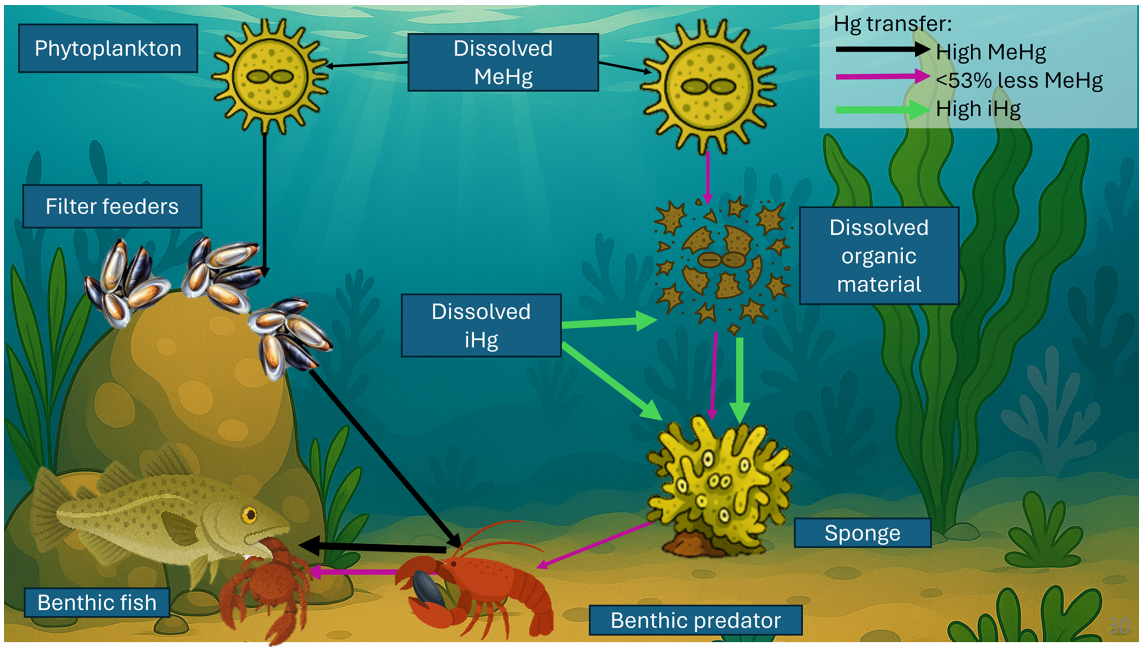

Figure 8. HMA sponges accumulate high iHg and low MeHg because they feed on DOM. The model indicates that these reduced MeHg levels at the food-web base can lower MeHg in fish by up to 53 %.

and MeHg concentrations are consistent with observations by Cossa et al. (2017), and MeHg bioaccumulation falls within the range reported by Llull et al. (2017); Tesán Onrubia et al. (2020). We ran the simulations assuming both that rDOM influences the ecosystem and Hg cycling, and assuming that rDOM is unreactive and does not play a key role. Our model and its comparison to the observations by Orani et al. (2020) demonstrate that several mechanisms could explain the observed Hg dynamics in Mediterranean sponges:

- DOM consumption provides a viable explanation for low MeHg in LMA sponges.
- The difference between MeHg bioaccumulation in LMA and HMA sponges can result from the consumption of rDOM by HMA sponges, or an in vivo demethylation rate of 1 % d^{-1} in HMA sponges.
- The consumption of DOM by sponges contributes to elevated iHg levels, but this mechanism alone is insufficient to explain the extremely high iHg concentrations observed in both LMA and HMA sponges. This suggests that sponges either have increased uptake or a reduced release rate of iHg. We present evidence to support the hypothesis that the high iHg concentration in sponges is caused by a reduced release rate of iHg.
- As an alternative hypothesis, we demonstrate that if sponges have elevated iHg and MeHg uptake rates, a demethylation rate of 13 % d^{-1} would be required, providing a loosely constrained upper bound for demethylation.
- Finally, our model suggests that MeHg bioaccumulation in benthic fish can be lower in a sponge-dominated system than in a comparable ecosystem without HMA sponges, with reductions of up to 53 %.

It must be noted that there is large unconstrained uncertainty in all results presented. This study should be seen as a hypothesis-generating modeling study rather than an exact quantification or verification of the proposed mechanisms. Targeted empirical research is needed to better understand the role of sponges in Hg cycling. However, based on our results, we propose that DOM-consuming sponges might play a key role in reducing MeHg bioaccumulation in benthic fish.

Appendix A: Equations for statistical metrics

The metrics for statistcal analyses are shown in Table A1 and the weighted mean of the modeled biomass and bioaccumulation of iHg and MeHg is shown in Table A2.

Table A1. Formulas for statistical metrics used to evaluate model. x_i and y_i are the modeled and observed values, respectively, n is the number of data points, and $\bar{x}$ is the modeled mean and $\bar{y}$ the observed mean.

Metric	Formula
Root Mean Square Error (RMSE)	$\mathrm{RMSE} = \sqrt{\frac{1}{n}\sum_{i=1}^{n}(x_i - y_i)^2}$
Pearson correlation coefficient r	$r = \frac{\sum_{i=1}^{n}(x_i-\bar{x})(y_i-\bar{y})}{\sqrt{\sum_{i=1}^{n}(x_i-\bar{x})^2}\sqrt{\sum_{i=1}^{n}(y_i-\bar{y})^2}}$
Standard deviation σ	$\sigma = \sqrt{\frac{1}{n}\sum_{i=1}^{n}(x_i - \bar{x})^2}$
Bias	$\mathrm{Bias} = \frac{1}{n}\sum_{i=1}^{n}(x_i - y_i)$
Mean Percent Bias (MPB)	$\mathrm{MPB} = 100 \times \frac{\bar{x}-\bar{y}}{\bar{y}}$
Kolmogorov–Smirnov (K-S) p-value	Two-sample test comparing the empirical distributions of x and y; p-value indicates the probability that both samples are drawn from the same distribution.

Table A2. Mean biomass and mercury bioaccumulation for all functional groups across the three main model setups investigated in this study. Benthic biomass is reported in mgC m^{-2}, while pelagic biomass (phytoplankton and zooplankton) is reported in mgC m^{-3}. Inorganic mercury (iHg) and methylmercury (MeHg) bioaccumulation are expressed in ng Hg mgC^{-1}. Bioaccumulation values are omitted when mean biomass was negligible (< 0).

	Biomass		MeHg		iHg	
	Mean	SD	Mean	SD	Mean	SD
Base Case						
Generalist feeder	256	177	37	8	69	8
Deposit feeder	1741	614	61	16	80	9
Filter feeder	158	118	35	11	59	10
HMA sponge	252	82	29	6	162	37
LMA sponge	1375	692	27	9	111	19
Predator	382	425	79	14	63	6
Benthic fish	226	231	422	524	57	10
Microzooplankton	16	26	12	4	32	21
Mesozooplankton	25	23	13	4	49	13
Phytoplankton	41	32	2	4	1	3
2.5 gC rDOM m^{-3}						
Generalist feeder	335	287	48	22	64	10
Deposit feeder	1186	797	97	44	82	12
Filter feeder	0	0	–	–	–	–
HMA sponge	6649	4388	13	6	82	10
LMA sponge	21	29	71	14	71	11
Predator	2578	4204	32	22	56	7
Benthic fish	963	1482	205	1614	56	15
Microzooplankton	18	22	17	9	32	18
Mesozooplankton	12	12	23	11	50	11
Phytoplankton	30	25	4	8	2	4
2.5 gC rDOM m^{-3} (No HMA)						
Generalist feeder	287	169	36	8	68	8
Deposit feeder	1568	659	53	13	79	6
Filter feeder	204	134	35	12	57	12
HMA sponge	0	0	–	–	–	–
LMA sponge	660	495	18	5	72	9
Predator	385	567	71	17	55	7
Benthic fish	179	209	437	360	51	13
Microzooplankton	19	28	13	4	32	18
Mesozooplankton	20	19	15	7	47	10
Phytoplankton	39	33	3	6	2	3

Code availability. The model code is publicly available via Amptmeijer (2026) (https://doi.org/10.5281/zenodo.19880931). All model data can be reproduced by downloading the code and following the instructions provided in the README file.

Data availability. No additional datasets are associated with this study other than reproducible model output data generated using the model code archived on Zenodo (https://doi.org/10.5281/zenodo.19880931, Amptmeijer, 2026).

Author contributions. DA, JB, UH, and CS were responsible for the conceptualisation of the study. DA, UH, JB and DA were responsible for the methodology. DA oversaw the evaluation of the model performance and performed statistical tests on the observations. DA wrote the original draft, and UH, JB, and DA conducted the review and quality control. JB was responsible for funding acquisition.

Competing interests. At least one of the (co-)authors is a member of the editorial board of *Biogeosciences*. The peer-review process was guided by an independent editor, and the authors also have no other competing interests to declare.

Disclaimer. Publisher's note: Copernicus Publications remains neutral with regard to jurisdictional claims made in the text, published maps, institutional affiliations, or any other geographical representation in this paper. The authors bear the ultimate responsibility for providing appropriate place names. Views expressed in the text are those of the authors and do not necessarily reflect the views of the publisher.

Acknowledgements. Readability suggestions for this paper were generated using gAI tools such as ChatGPT (OpenAI), while AI-based spell checks such as Grammarly and Writefull were used to correct spelling. In addition, AI tools helped optimize the R and Python scripts and provide coding suggestions. All suggestions were implemented only after critical manual evaluation. Finally, Google Scholar and Perplexity were used to find sources for literature research, which were consequently manually read, verified, and cited. Several sub-images were generated that together compose the key figure; these were generated using openART and GPT-4.1.

Financial support. This research has been supported by the HORIZON EUROPE Marie Sklodowska-Curie Actions (grant no. 860497).

The article processing charges for this open-access publication were covered by the Helmholtz-Zentrum Hereon.

Review statement. This paper was edited by Xun Wang and reviewed by two anonymous referees.

References

Amptmeijer, D. J.: Model_code_MERCY_ECOSMO-Sponge_Bioaccumulation, Zenodo [code], https://doi.org/10.5281/zenodo.19880931, 2026.

Amptmeijer, D. J., Mikheeva, E., Daewel, U., Bieser, J., and Schrum, C.: Bioaccumulation as a driver of high MeHg in the North and Baltic Seas, Biogeosciences, 22, 7929–7960, https://doi.org/10.5194/bg-22-7929-2025, 2025a.

Amptmeijer, D. J., Padilla, A., Modesti, S., Schrum, C., and Bieser, J.: Feeding strategy as a key driver of the bioaccumulation of MeHg in megabenthos, Biogeosciences, 22, 7483–7503, https://doi.org/10.5194/bg-22-7483-2025, 2025b.

Baltar, F., Alvarez-Salgado, X. A., Arístegui, J., Benner, R., Hansell, D. A., Herndl, G. J., and Lønborg, C.: What Is Refractory Organic Matter in the Ocean?, Front. Mar. Sci., 8, https://doi.org/10.3389/fmars.2021.642637, 2021.

Bart, M. C., de Kluijver, A., Hoetjes, S., Absalah, S., Mueller, B., Kenchington, E., Rapp, H. T., and de Goeij, J. M.: Differential processing of dissolved and particulate organic matter by deep-sea sponges and their microbial symbionts, Sci. Rep., 10, 1–13, https://doi.org/10.1038/s41598-020-74670-0, 2020.

Bart, M. C., Mueller, B., Rombouts, T., van de Ven, C., Tompkins, G. J., Osinga, R., Brussaard, C. P., MacDonald, B., Engel, A., Rapp, H. T., and de Goeij, J. M.: Dissolved organic carbon (DOC) is essential to balance the metabolic demands of four dominant North-Atlantic deep-sea sponges, Limnol. Oceanogr., 66, 925–938, https://doi.org/10.1002/LNO.11652, 2021.

Belgacem, M., Schroeder, K., Barth, A., Troupin, C., Pavoni, B., Raimbault, P., Garcia, N., Borghini, M., and Chiggiato, J.: Climatological distribution of dissolved inorganic nutrients in the western Mediterranean Sea (1981–2017), Earth Syst. Sci. Data, 13, 5915–5949, https://doi.org/10.5194/essd-13-5915-2021, 2021.

Bellanger, M., Pichery, C., Aerts, D., Berglund, M., Castaño, A., Čejchanová, M., Crettaz, P., Davidson, F., Esteban, M., Fischer, M. E., Gurzau, A. E., Halzlova, K., Katsonouri, A., Knudsen, L. E., Kolossa-Gehring, M., Koppen, G., Ligocka, D., Miklavčič, A., Reis, M. F., Rudnai, P., Tratnik, J. S., Weihe, P., Budtz-Jorgensen, E., and Grandjean, P.: Economic benefits of methylmercury exposure control in Europe: monetary value of neurotoxicity prevention, in: Environmental health: a global access science source, 12, https://doi.org/10.1186/1476-069X-12-3, 2013.

Bertolino, M., Reboa, A., Armenio, C., Castellano, M., Felline, S., Terlizzi, A., and Bavestrello, G.: Sponges as feeding resource for the white seabream Diplodus sargus (Linnaeus, 1758) from the Mediterranean Sea, Eur. Zool. J., 91, 1192–1198, https://doi.org/10.1080/24750263.2024.2431084, 2024.

Bieser, J., Amptmeijer, D. J., Daewel, U., Kuss, J., Soerensen, A. L., and Schrum, C.: The 3D biogeochemical marine mercury cycling model MERCY v2.0 – linking atmospheric Hg to methylmercury in fish, Geosci. Model Dev., 16, 2649–2688, https://doi.org/10.5194/gmd-16-2649-2023, 2023.

Bolding, K., Bruggeman, J., Burchard, H., and Umlauf, L.: General Ocean Turbulence Model – GOTM, Zenodo [code], https://doi.org/10.5281/ZENODO.4896611, 2021.

Briant, N., Chouvelon, T., Martinez, L., Brach-Papa, C., Chiffoleau, J. F., Savoye, N., Sonke, J., and Knoery, J.: Spatial and temporal distribution of mercury and methylmercury in bivalves

from the French coastline, Mar. Pollut. Bull., 114, 1096–1102, https://doi.org/10.1016/j.marpolbul.2016.10.018, 2017.

Bruggeman, J. and Bolding, K.: A general framework for aquatic biogeochemical models, Environ. Model. Softw., 61, 249–265, https://doi.org/10.1016/J.ENVSOFT.2014.04.002, 2014.

Buckman, K. L., Seelen, E. A., Mason, R. P., Balcom, P., Taylor, V. F., Ward, J. E., and Chen, C. Y.: Sediment organic carbon and temperature effects on methylmercury concentration: a mesocosm experiment, Sci. Total Environ., 666, 1316, https://doi.org/10.1016/J.SCITOTENV.2019.02.302, 2019.

Claisse, D.: Chemical Contamination of French Coasts The Results of a Ten Years Mussel Watch, Mar. Pollut. Bull., https://doi.org/10.1016/0025-326X(89)90141-0, 1989.

Cossa, D., Durrieu de Madron, X., Schäfer, J., Lanceleur, L., Guédron, S., Buscail, R., Thomas, B., Castelle, S., and Naudin, J. J.: The open sea as the main source of methylmercury in the water column of the Gulf of Lions (Northwestern Mediterranean margin), Geochim. Cosmochim. Acta, 199, 222–237, https://doi.org/10.1016/J.GCA.2016.11.037, 2017.

Cruz, K., Guézennec, J., and Barkay, T.: Binding of Hg by bacterial extracellular polysaccharide: a possible role in Hg tolerance, Appl. Microbiol. Biotechnol., 101, 5493–5503, https://doi.org/10.1007/s00253-017-8239-z, 2017.

da Cruz, J. F., Gaspar, H., and Calado, G.: Turning the game around: Toxicity in a nudibranch-sponge predator-prey association, Chemoecology, 22, 47–53, https://doi.org/10.1007/S00049-011-0097-Z, 2012.

Daewel, U. and Schrum, C.: Simulating long-term dynamics of the coupled North Sea and Baltic Sea ecosystem with ECOSMO II: Model description and validation, J. Mar. Syst., 119-120, 30–49, https://doi.org/10.1016/J.JMARSYS.2013.03.008, 2013.

Daewel, U., Schrum, C., and Macdonald, J. I.: Towards end-to-end (E2E) modelling in a consistent NPZD-F modelling framework (ECOSMO E2E_v1.0): application to the North Sea and Baltic Sea, Geosci. Model Dev., 12, 1765–1789, https://doi.org/10.5194/gmd-12-1765-2019, 2019.

De Goeij, J. M., Van Oevelen, D., Vermeij, M. J., Osinga, R., Middelburg, J. J., De Goeij, A. F., and Admiraal, W.: Surviving in a marine desert: The sponge loop retains resources within coral reefs, Science, 342, 108–110, https://doi.org/10.1126/SCIENCE.1241981, 2013.

Dolan, J. R.: The History of Biological Exploration of the Bay of Villefranche, Protist, 165, 636–644, https://doi.org/10.1016/J.PROTIS.2014.07.005, 2014.

Dutton, J. and Fisher, N. S.: Bioavailability of sediment-bound and algal metalsto killifish Fundulus heteroclitus, Aquat. Biol., 16, 85–96, https://doi.org/10.3354/ab00437, 2012.

Erwin, P. M., Coma, R., Serrano, E., and Ribes, M.: Stable symbionts across the HMA-LMA dichotomy: low seasonal and interannual variation in sponge-associated bacteria from taxonomically diverse hosts, FEMS Microbiol. Ecol., 91, https://doi.org/10.1093/femsec/fiv115, 2015.

Esteves, A. I., Nicolai, M., Humanes, M., and Goncalves, J.: Sulfated polysaccharides in marine sponges: Extraction methods and anti-HIV activity, Mar. Drugs, 9, 139–153, https://doi.org/10.3390/md9010139, 2011.

Fonds, M., Cronie, R., Vethaak, A. D., and Van Der Puyl, P.: Metabolism, food consumption and growth of plaice (Pleuronectes platessa) and flounder (Platichthys flesus) in relation to fish size and temperature, Neth. J. Sea Res., 29, 127–143, https://doi.org/10.1016/0077-7579(92)90014-6, 1992.

Fromentin, J.-M., Dauvin, J.-C., Ibanez, F., Dewarumez, J.-M., and Elkaim, B.: Long-term variations of four macrobenthic community structures, Oceanolica Acta, 20, 43–53, https://archimer.ifremer.fr/doc/00093/20407/ (last access: 20 May 2026), 1997.

Garcia, H. E., Boyer, T. P., Baranova, O. K., Locarnini, R. A., Mishonov, A. V., Grodsky, A., Paver, C. R., Weathers, K. W., Smolyar, I. V., Reagan, J. R., Seidov, D., and Zweng, M. W.: World Ocean Atlas 2018: Product Documentation, edited by: Mishonov, A., https://doi.org/10.25923/tzyw-rp36, 2019.

Garcia-Arevalo, I., Berard, J.-B., Bieser, J., Le Faucheur, S., Hubert, C., Lacour, T., Thomas, B., Cossa, D., and Knoery, J.: Mercury Accumulation Pathways in a Model Marine Microalgae: Sorption, Uptake, and Partition Kinetics, ACS ES&T Water, 4, 2826–2835, https://doi.org/10.1021/acsestwater.3c00795, 2024.

García-Bonilla, E., Brandão, P. F. B., Pérez, T., and Junca, H.: Stable and Enriched Cenarchaeum symbiosum and Uncultured Betaproteobacteria HF1 in the Microbiome of the Mediterranean Sponge Haliclona fulva (Demospongiae: Haplosclerida), Microb. Ecol., 77, 25–36, https://doi.org/10.1007/s00248-018-1201-5, 2019.

GEBCO Bathymetric Compilation Group: The GEBCO_2020 Grid – a continuous terrain model of the global oceans and land, Tech. rep., British Oceanographic Data Centre, National Oceanography Centre, NERC, UK, https://doi.org/10.5285/a29c5465-b138-234d-e053-6c86abc040b9, 2020.

Gloeckner, V., Wehrl, M., Moitinho-Silva, L., Gernert, C., Schupp, P., Pawlik, J. R., Lindquist, N. L., Erpenbeck, D., Wörheide, G., Wörheide, W., and Hentschel, U.: The HMA-LMA Dichotomy Revisited: an Electron Microscopical Survey of 56 Sponge Species, Biol. Bull., 227, 78–88, https://doi.org/10.1086/BBLv227n1p78, 2014.

Graham, A. M., Aiken, G. R., and Gilmour, C. C.: Dissolved Organic Matter Enhances Microbial Mercury Methylation Under Sulfidic Conditions, Environ. Sci. Technol, 46, 29, https://doi.org/10.1021/es203658f, 2012.

Hanz, U., Riekenberg, P., de Kluijver, A., van der Meer, M., Middelburg, J. J., de Goeij, J. M., Bart, M. C., Wurz, E., Colaço, A., Duineveld, G. C. A., Reichart, G.-J., Rapp, H.-T., and Mienis, F.: The important role of sponges in carbon and nitrogen cycling in a deep-sea biological hotspot, Funct. Ecol., 36, 2188–2199, https://doi.org/10.1111/1365-2435.14117, 2022.

Hao, Y. Y., Zhu, Y. J., Yan, R. Q., Gu, B., Zhou, X. Q., Wei, R. R., Wang, C., Feng, J., Huang, Q., and Liu, Y. R.: Important Roles of Thiols in Methylmercury Uptake and Translocation by Rice Plants, Environ. Sci. Technol., 56, 6765–6773, https://doi.org/10.1021/ACS.EST.2C00169, 2022.

Hentschel, U., Usher, K. M., and Taylor, M. W.: Marine sponges as microbial fermenters, FEMS Microbiol. Ecol., 55, 167–177, https://doi.org/10.1111/j.1574-6941.2005.00046.x, 2006.

Hentschel, U., Piel, J., Degnan, S. M., and Taylor, M. W.: Genomic insights into the marine sponge microbiome, Nat. Rev. Microbiol., 10, 641–654, https://doi.org/10.1038/NRMICRO2839, 2012.

Jeong, H., Ali, W., Zinck, P., Souissi, S., and Lee, J. S.: Toxicity of methylmercury in aquatic organisms and interaction with environmental factors and coexisting pollutants: A review, Sci. Total Environ., 943, https://doi.org/10.1016/j.scitotenv.2024.173574, 2024.

Koopmans, M. and Wijffels, R. H.: Seasonal Growth Rate of the Sponge Haliclona oculata (Demospongiae: Haplosclerida), Mar. Biotechnol. (NY), 10, 502, https://doi.org/10.1007/S10126-008-9086-9, 2008.

Labrune, C., Grémare, A., Amouroux, J. M., Sardá, R., Gil, J., and Taboada, S.: Assessment of soft-bottom polychaete assemblages in the Gulf of Lions (NW Mediterranean) based on a mesoscale survey, Estuar. Coast. Shelf Sci., 71, 133–147, https://doi.org/10.1016/J.ECSS.2006.07.007, 2007.

Lavoie, R. A., Jardine, T. D., Chumchal, M. M., Kidd, K. A., and Campbell, L. M.: Biomagnification of Mercury in Aquatic Food Webs: A Worldwide Meta-Analysis, https://doi.org/10.1021/es403103t, 2013.

Lee, C. S. and Fisher, N. S.: Methylmercury uptake by diverse marine phytoplankton, Limnol. Oceanogr., 61, 1626–1639, https://doi.org/10.1002/lno.10318, 2016.

Llull, R. M., Garí, M., Canals, M., Rey-Maquieira, T., and Grimalt, J. O.: Mercury concentrations in lean fish from the Western Mediterranean Sea: Dietary exposure and risk assessment in the population of the Balearic Islands, Environ. Res., 158, 16–23, https://doi.org/10.1016/j.envres.2017.05.033, 2017.

Lønborg, C., Carreira, C., Abril, G., Agustí, S., Amaral, V., Andersson, A., Arístegui, J., Bhadury, P., Bif, M. B., Borges, A. V., Bouillon, S., Calleja, M. L., Cotovicz, L. C., Cozzi, S., Doval, M., Duarte, C. M., Eyre, B., Fichot, C. G., García-Martín, E. E., Garzon-Garcia, A., Giani, M., Gonçalves-Araujo, R., Gruber, R., Hansell, D. A., Hashihama, F., He, D., Holding, J. M., Hunter, W. R., Ibánhez, J. S. P., Ibello, V., Jiang, S., Kim, G., Klun, K., Kowalczuk, P., Kubo, A., Lee, C. W., Lopes, C. B., Maggioni, F., Magni, P., Marrase, C., Martin, P., McCallister, S. L., McCallum, R., Medeiros, P. M., Morán, X. A. G., Muller-Karger, F. E., Myers-Pigg, A., Norli, M., Oakes, J. M., Osterholz, H., Park, H., Lund Paulsen, M., Rosentreter, J. A., Ross, J. D., Rueda-Roa, D., Santinelli, C., Shen, Y., Teira, E., Tinta, T., Uher, G., Wakita, M., Ward, N., Watanabe, K., Xin, Y., Yamashita, Y., Yang, L., Yeo, J., Yuan, H., Zheng, Q., and Álvarez-Salgado, X. A.: A global database of dissolved organic matter (DOM) concentration measurements in coastal waters (CoastDOM v1), Earth Syst. Sci. Data, 16, 1107–1119, https://doi.org/10.5194/essd-16-1107-2024, 2024.

Maldonado, M. and Uriz, M. J.: Microrefuge exploitation by subtidal encrusting sponges: patterns of settlement and post-settlement survival, Mar. Ecol. Prog. Ser., 174, 141–150, 1998.

Mason, R. P., Reinfelder, J. R., and Morel, F. M.: Bioaccumulation of mercury and methylmercury, Water Air Soil Pollut., 80, 915–921, https://doi.org/10.1007/BF01189744, 1995.

Mason, R. P., Reinfelder, J. R., and Morel, F. M.: Uptake, toxicity, and trophic transfer of mercury in a coastal diatom, Environ. Sci. Technol., 30, 1835–1845, https://doi.org/10.1021/es950373d, 1996.

Mathema, V. B., Thakuri, B. C., and Sillanpää, M.: Bacterial mer operon-mediated detoxification of mercurial compounds: A short review, Arch. Microbiol., 193, 837–844, https://doi.org/10.1007/s00203-011-0751-4, 2011.

Menden-Deuer, S., and Lessard, E. J.: Carbon to volume relationships for dinoflagellates, diatoms, and other protist plankton, Limnol. Oceanogr., 45, 569–579, https://doi.org/10.4319/lo.2000.45.3.0569, 2000.

Morel, F. M. M., Kraepiel, A. M. L., and Amyot, M.: The Chemical Cycle and Bioaccumulation of Mercury, Annu. Rev. Ecol. Syst., 29, 543–566, https://www.jstor.org/stable/221718?seq=1&cid=pdf-, 1998.

Mortimer, C., Dunn, M., Haris, A., Jompa, J., and Bell, J.: Estimates of sponge consumption rates on an Indo-Pacific reef, Mar. Ecol. Prog. Ser., 672, 123–140, https://doi.org/10.3354/MEPS13786, 2021.

Orani, A. M., Vassileva, E., Azemard, S., and Thomas, O. P.: Comparative study on Hg bioaccumulation and biotransformation in Mediterranean and Atlantic sponge species, Chemosphere, 260, 127515, https://doi.org/10.1016/J.CHEMOSPHERE.2020.127515, 2020.

Pacyna, E. G., Pacyna, J. M., Steenhuisen, F., and Wilson, S.: Global anthropogenic mercury emission inventory for 2000, Atmos. Environ., 40, 4048–4063, https://doi.org/10.1016/j.atmosenv.2006.03.041, 2006.

Pan, K. and Wang, W. X.: Mercury accumulation in marine bivalves: Influences of biodynamics and feeding niche, Environ. Pollut., 159, 2500–2506, https://doi.org/10.1016/J.ENVPOL.2011.06.029, 2011.

Perger, R. and Temming, A.: A new method to determine in situ growth rates of decapod shrimp: A case study with brown shrimp Crangon crangon, Mar. Biol., 159, 1209–1222, https://doi.org/10.1007/s00227-012-1901-1, 2012.

Regnault, M.: Respiration and Ammonia Excretion of the Shrimp Crangon crangon L.: Metabolic Response to Prolonged Starvation, J. Comp. Physiol, 141, 549–555, https://doi.org/10.1007/BF01101478, 1981.

REPHY: Time Series: REPHY Villefranche https://www.st.nmfs.noaa.gov/copepod/time-series/fr-50114/ (last access: 20 May 2026), 2020.

Ribes, M., Coma, R., and Gili, J. M.: Seasonal variation of particulate organic carbon, dissolved organic carbon and the contribution of microbial communities to the live particulate organic carbon in a shallow near-bottom ecosystem at the Northwestern Mediterranean Sea, J. Plankton Res., 21, 1077–1100, https://doi.org/10.1093/plankt/21.6.1077, 1999.

Rijsgard, H. and Banta, G.: Irrigation and deposit feeding by the lugworm Arenicula marina, characteristics and secondary effects on the environment. A review of current knowledge., Vie Milieu - Life Environ., 4, 243–257, https://hal.sorbonne-universite.fr/hal-03173003 (last access: 20 May 2026), 1998.

Rodil, I. F., Attard, K. M., Norkko, J., Glud, R. N., and Norkko, A.: Estimating Respiration Rates and Secondary Production of Macrobenthic Communities Across Coastal Habitats with Contrasting Structural Biodiversity, Ecosystems, 23, 630–647, https://doi.org/10.1007/s10021-019-00427-0, 2019.

Rosenberg, R., Grémare, A., Amouroux, J.-M., and Nilsson, H. C.: Benthic habitats in the northwest Mediterranean characterised by sedimentary organics, benthic macrofauna and sediment profile images, Estuar. Coast. Shelf Sci., 297–311, https://doi.org/10.1016/S0272-7714(02)00356-6, 2003.

Santos-Gandelman, J. F., Giambiagi-Demarval, M., Muricy, G., Barkay, T., and Laport, M. S.: Mercury and methylmercury detoxification potential by sponge-associated bacteria, Antonie van Leeuwenhoek, 585–590, https://doi.org/10.1007/s10482-014-0224-2, 2014.

Schartup, A. T., Ndu, U., Balcom, P. H., Mason, R. P., and Sunderland, E. M.: Contrasting Effects of Marine and Terrestrially Derived Dissolved Organic Matter on Mercury Speciation and Bioavailability in Seawater, Environ. Sci. Technol., 49, 5965–5972, https://doi.org/10.1021/es506274x, 2015.

Seelen, E., Liem-Nguyen, V., Wünsch, U., Baumann, Z., Mason, R., Skyllberg, U., and Björn, E.: Dissolved organic matter thiol concentrations determine methylmercury bioavailability across the terrestrial-marine aquatic continuum, Nat. Comm., 14, https://doi.org/10.1038/s41467-023-42463-4, 2023.

Sicko-Goad, L. M., Schelske, C. L., and Stoermer, E. F.: Estimation of intracellular carbon and silica content of diatoms from natural assemblages using morphometric techniques, Limnol. Oceanogr, 29, 1170–178, https://doi.org/10.4319/lo.1984.29.6.1170, 1984.

Storelli, M. M., Stuffler, R. G., and Marcotrigiano, G. O.: Total and methylmercury residues in tuna-fish from the Mediterranean sea, Food Addit. Contam., 19, 715–720, https://doi.org/10.1080/02652030210153569, 2002.

Tesán Onrubia, J. A., Petrova, M. V., Puigcorbé, V., Black, E. E., Valk, O., Dufour, A., Hamelin, B., Buesseler, K. O., Masqué, P., Le Moigne, F. A., Sonke, J. E., Rutgers Van Der Loeff, M., and Heimbürger-Boavida, L. E.: Mercury Export Flux in the Arctic Ocean Estimated from 234Th/238U Disequilibria, ACS Earth Space Chem., 4, 795–801, https://doi.org/10.1021/acsearthspacechem.0c00055, 2020.

Tesán-Onrubia, J. A., Heimbürger-Boavida, L. E., Dufour, A., Harmelin-Vivien, M., García-Arévalo, I., Knoery, J., Thomas, B., Carlotti, F., Tedetti, M., and Bănaru, D.: Bioconcentration, bioaccumulation and biomagnification of mercury in plankton of the Mediterranean Sea, Mar. Pollut. Bull., 194, 115439, https://doi.org/10.1016/J.MARPOLBUL.2023.115439, 2023.

Thiel, V., Leininger, S., Schmaljohann, R., Brümmer, F., and Imhoff, J. F.: Sponge-specific Bacterial Associations of the Mediterranean Sponge Chondrilla nucula (Demospongiae, Tetractinomorpha), Microb. Ecol., 54, 101–111, https://doi.org/10.1007/s00248-006-9177-y, 2007.

Thomassen, S. and Riisgadrd, H. U.: Growth and energetics of the sponge Halichondria panicea, Mar. Ecol. Prog. Ser., 128, 239–246, https://doi.org/10.3354/meps128239, 1995.

Tseng, C.-M., Ang, S.-J., Chen, Y.-S., Shiao, J.-C., Lamborg, C. H., He, X., and Reinfelder, J. R.: Bluefin tuna reveal global patterns of mercury pollution and bioavailability in the world's oceans, PNAS, 118, https://doi.org/10.1073/pnas.2111205118, 2021.

Tsui, M. T. and Wang, W. X.: Uptake and Elimination Routes of Inorganic Mercury and Methylmercury in Daphnia magna, Environ. Sci. Technol., 38, 808–816, https://doi.org/10.1021/es034638x, 2004.

Vacelet, J. and Donadey, C.: Electron microscope study of the association between some sponges and bacteria, J. Exp. Mar. Biol. Ecol., 30, 301–314, https://doi.org/10.1016/0022-0981(77)90038-7, 1977.

Vilanova, E., Zilberberg, C., Kochem, M., Custodio, M. R., and Mourão, P. A. S.: A novel biochemical method to distinguish cryptic species of Chondrilla (Chondrosida, Demospongiae) based on its sulfated polysaccharides, Porifera Research: Biodiversity, Innovation and Sustainability, 653–659, https://www.researchgate.net/profile/Marcio-Custodio-2/publication/257954142_Porifera_Research_Biodiversity_Innovation_and_Sustainability/links/0deec526798bb07302000000/Porifera-Research-Biodiversity-Innovation-and-Sustainability.pdf#page=663 (last access: 20 May 2026), 2007.

Wallace, J. C.: Feeding, Starvation and Metabolic Rate in the Shore Crab Carcinus maenas, Mar. Biol., 20, 227–281, https://doi.org/10.1007/BF00354271, 1973.

Webster, N. S. and Thomas, T.: The sponge hologenome, mBio, 7, 135–151, https://doi.org/10.1128/mbio.00135-16, 2016.

Weisz, J. B., Lindquist, N., and Martens, C. S.: Do associated microbial abundances impact marine demosponge pumping rates and tissue densities?, Oecologia, 155, 367–376, https://doi.org/10.1007/S00442-007-0910-0, 2008.

Wouters, H., Berckmans, J., Maes, R., Vanuytrecht, E., and De Ridder, K.: Global bioclimatic indicators from 1979 to 2018 derived from reanalysis, version 1.0, Copernicus Climate Change Service (C3S) Climate Data Store (CDS), https://doi.org/10.24381/cds.bce175f0, 2021.

Wu, P., Kainz, M. J., Bravo, A. G., Åkerblom, S., Sonesten, L., and Bishop, K.: The importance of bioconcentration into the pelagic food web base for methylmercury biomagnification: A meta-analysis, Sci. Total Environ., 646, 357–367, https://doi.org/10.1016/j.scitotenv.2018.07.328, 2019.